NASA TECHNICAL NOTE

NASA TN D-2492

NASA TN D-2492

LOW-SPEED FORCE AND FLIGHT INVESTIGATION OF A MODEL OF A MODIFIED PARAWING UTILITY VEHICLE

by Joseph L. Johnson, Jr.

Langley Research Center
Langley Station, Hampton, Va.

NATIONAL AERONAUTICS AND SPACE ADMINISTRATION • WASHINGTON, D. C. • MARCH 1965

NASA TN D-2492

LOW-SPEED FORCE AND FLIGHT INVESTIGATION OF A MODEL OF A MODIFIED PARAWING UTILITY VEHICLE

By Joseph L. Johnson, Jr.

Langley Research Center
Langley Station, Hampton, Va.

Technical Film Supplement L-836 available on request.

NATIONAL AERONAUTICS AND SPACE ADMINISTRATION

For sale by the Office of Technical Services, Department of Commerce,
Washington, D.C. 20230 -- Price $3.00

LOW-SPEED FORCE AND FLIGHT INVESTIGATION OF A MODEL OF A MODIFIED PARAWING UTILITY VEHICLE

By Joseph L. Johnson, Jr.

SUMMARY

A low-speed wind-tunnel investigation has been made to determine the flight characteristics of a model of a parawing utility vehicle. The model was generally similar in design to an earlier model of a parawing utility vehicle flight tested, but incorporated several design changes, primarily in the area of control, which were intended to correct certain deficiencies of the earlier vehicle. Included in the modifications was a 35° vee-tail installed to provide pitch and yaw control. In addition, the aft 14 percent of each leading edge of the parawing was hinged to deflect with wing bank much like a servo tab in an effort to reduce the large lateral hinge moments associated with the wing-bank control system.

The results of the investigation showed that the model had generally satisfactory stability characteristics over the angle-of-attack range covered in the flight tests, but force tests showed that it had a pitch-up tendency at angles of attack above those covered in the flight tests. The control effectiveness provided by the design control system was unsatisfactory about each of the three axes in some flight conditions. A revised control system was devised, however, which gave satisfactory control.

INTRODUCTION

In connection with a general research program being conducted by the National Aeronautics and Space Administration to provide some basic information on configurations employing the parawing concept, a low-speed force and flight investigation has been conducted in the Langley full-scale tunnel on a model of a modified parawing utility vehicle. The model was generally similar in design to the parawing utility vehicle flight tested in a previous investigation (see ref. 1), but incorporated several design changes which were intended to correct certain deficiencies of the earlier vehicle. The modified vehicle was similar to the earlier vehicle in that it consisted basically of a cargo platform attached to a parawing by means of an overhead truss arrangement. It was powered by a pusher propeller located at the aft end of the platform and had a cockpit located at the front. The original vehicle was controlled by banking and pitching the wing. In the design configuration of the present vehicle, wing bank was still used for roll control, but the aft 14 percent of each leading edge of the parawing was hinged, much like a servo tab, in an effort to reduce

the large hinge moments associated with the wing-bank control system. A 35° vee-tail was mounted behind the propeller, outside the propeller disk, and control surfaces on the vee-tail were used to provide pitch and yaw control.

The present investigation was made to determine the static and dynamic stability and the control characteristics of the modified vehicle. Flight tests were made over an angle-of-attack range of the parawing keel from about 20° up to the maximum trim angle of attack possible (31°) with the design control system. Tests were also made with the revised control system. Static force tests were made over a keel angle-of-attack range from 0° to 45° to determine the static stability and control characteristics of the model for correlation with the flight-test results.

Motion-picture supplement L-836 has been prepared and is available on loan. A request card and a description of the film are included at the back of this document.

SYMBOLS

All forces, moments, and velocities with the exception of lift and drag are presented with respect to a system of body axes originating at the reference center-of-gravity position shown in figures 1 and 2. All measurements are reduced to standard coefficient form and are based on the dimensional characteristics of the flat planform of the parawing (45° leading-edge sweep).

b	wing span, ft
c_k	parawing keel length, ft
C_D	drag coefficient, F_D/qS
C_h	hinge-moment coefficient, M_h/qSb
C_L	lift coefficient, F_L/qS
C_l	rolling-moment coefficient, M_X/qSb
C_m	pitching-moment coefficient, M_Y/qSc_k
C_n	yawing-moment coefficient, M_Z/qSb
C_Y	lateral-force coefficient, F_Y/qS

$C_{l_\beta} = \frac{\partial C_l}{\partial \beta}$, per deg

$C_{n_\beta} = \frac{\partial C_n}{\partial \beta}$, per deg

$C_{Y_\beta} = \frac{\partial C_Y}{\partial \beta}$, per deg

F_D drag, lb

F_L lift, lb

F_Y side force, lb

I_X moment of inertia about X-axis, slug-ft^2

I_Y moment of inertia about Y-axis, slug-ft^2

I_Z moment of inertia about Z-axis, slug-ft^2

i_t angle of incidence of horizontal tail, positive when trailing edge down, deg

i_w angle of incidence of parawing keel with respect to platform, $\alpha_k - \alpha_p$, deg

L/D lift-drag ratio

M_h hinge moment (positive when M_h tends to deflect wing-tip trailing edge downward), ft-lb

M_X rolling moment, ft-lb

M_Y pitching moment, ft-lb

M_Z yawing moment, ft-lb

q free-stream dynamic pressure, lb/sq ft

S wing area, sq ft

S_t tail area, sq ft

T_c thrust coefficient,

$$\left[C_{D_{(\text{power on})}} - C_{D_{(\text{power off, propeller windmilling})}}\right]_{\alpha_p = 0^\circ}$$

X,Y,Z longitudinal, lateral, and normal body axes, respectively

x,z	distances along X-axis and Z-axis, respectively, ft
α_k	angle of attack of keel, deg
α_p	angle of attack of platform, deg
β	angle of sideslip, deg
δ_e	deflection of elevator surface, positive when trailing edge down, deg
δ_r	deflection of rudder surfaces, positive when trailing edge left, deg
δ_{tip}	deflection of hinged wing tips, positive when trailing edge down, deg
ϕ	angle of roll (bank) of wing, positive when right wing tip down, deg

MODEL AND APPARATUS

The test vehicle used in the investigation was a 1/3-scale model of a light utility STOL aircraft. The configuration was generally similar in design to the original airplane described in references 1 and 2, but had several modifications which were intended to improve the aircraft handling qualities. A three-view drawing of the model with the design vee-tail arrangement and with a modified tail arrangement is presented in figure 2(a) and figure 2(b), respectively. A sketch of the linkage used in the design control system is shown in figure 2(c) and photographs of the model are presented in figure 3. Dimensional and mass characteristics of the model are presented in table I.

The modified vehicle was similar to the earlier vehicle in that it consisted basically of a cargo platform attached to a parawing by means of an overhead truss arrangement. It was powered by a pusher propeller located at the aft end of the platform and had a cockpit located at the front. The parawing used on the vehicle consisted of an aluminum-alloy box-beam keel and two airfoil-shaped leading edges hinged together at the apex of the wing. A fixed leading-edge sweep angle of 50° was maintained by a spreader bar which was attached to the parawing leading edges and to the keel at approximately the 44.5-percent keel station. The spreader bar was hinged to the top of a pyramid-type structure mounted on the platform and banked with the wing about an axis parallel to the platform. The fabric used to form the membrane of the parawing was made of nylon cloth with a plastic coating to give essentially zero porosity.

The original parawing utility vehicle was controlled by banking and pitching the wing (which is, in effect, control by center-of-gravity shift). Wing bank was still used for the design configuration of the present vehicle for roll control, but the aft 14 percent of each leading edge of the parawing was hinged, much like a servo tab, in an effort to reduce the large hinge moments associated with the wing-bank control system. The hinge axis of the wing tips was located so that the tips deflected in a plane parallel to the

wing surface at the maximum span location. When the wing was banked with this arrangement, one tip effectively moved inward and upward and the other outward and downward. In this control system, the roll cables from the roll actuator were linked directly to the hinged wing tips through a pulley-cable system along the spreader bar and wing leading edges. When the wing tips were deflected, they provided a rolling moment which, in turn, banked the wing. Centering springs were provided in this system to insure tension in the roll cables when the wing was not under air loads.

Pitch and yaw control were provided in the design configuration of the present vehicle by a 35° vee-tail arrangement mounted behind and below the pusher propeller. For some tests, a horizontal-tail and rudder arrangement mounted directly in the propeller slipstream was used for increased pitch and yaw control. (See fig. 2(b).) In some tests in which the rudder was installed the vee-tail was removed and in other tests it was left on. In all tests, longitudinal trim was achieved through variable wing incidence.

Electrically operated servoactuators mounted on the platform were used to provide control deflections in response to electrical signals generated by the pilot's control stick. The control used was similar to the full-off and full-on type in that a control signal deflected the surfaces at a fixed rate (depending upon the gearing and linkage involved). When the control stick was released, the control surfaces returned to their neutral setting.

Thrust for the model was supplied by a pneumatic motor driving a four-blade pusher propeller. The propeller blades were of 3-inch chord and were set at a blade angle of 14° measured at the 0.75-radius station.

The investigation was conducted in the Langley full-scale tunnel. The flight tests were made by using the technique given in reference 3 and the equipment illustrated in figure 4. Static force tests were made by using sting-type support equipment and strain-gage balances.

TESTS

Flight Tests

Flight tests were made to study the dynamic stability and control characteristics of the model over a keel angle-of-attack range from 20° up to the maximum trim angle of attack possible (31°). The model was flown with the vee-tail arrangement to provide pitch and yaw control and, in addition, was flown with a horizontal-tail and rudder arrangement mounted directly in the propeller slipstream to provide pitch and yaw control. In this tail arrangement (which was not force tested), the horizontal tail was identical in size to the rudder surface shown in figure 2(b). The model with the larger horizontal-tail arrangement shown in figure 2(b) and mentioned in the "Model and Apparatus" section was not flight tested. For a few tests, the model was flown with the wing tips deflected symmetrically to provide pitch control. For most flights, roll control was provided by the combination of wing bank and wing-tip deflection. A few tests were also made in which the wing tips were locked and roll

control was provided by pure wing bank. Other tests were made in which the wing was locked in bank and roll control was provided by differential deflection of the wing tips. Wing-bank angle used for lateral control was $\pm 5^{\circ}$ and wing-tip deflections varied from $\pm 10^{\circ}$ to $\pm 17^{\circ}$. Vee-tail rudder and elevator deflections were $\pm 12^{\circ}$ and $\pm 25^{\circ}$, respectively.

For all flight tests, the longitudinal location of the center of gravity was the same as that used for the force-test center-of-gravity reference shown in figure 2. The vertical location of the center of gravity for the flight tests was 2.67 inches above the reference axis shown in figure 2.

Force Tests

For all the force tests, the strain-gage balance was mounted so that its longitudinal axis was alined with the cargo platform. The balance moment center was located at the reference center of gravity shown in figure 2. Since the forces and moments were therefore measured with respect to the platform angle, it was more convenient to use this angle rather than the keel angle as a reference for angle of attack. For this reason, the data are plotted in terms of platform angle and are discussed in terms of this angle except for a few cases where the data are referred to the keel angle for comparison purposes.

Power-off and power-on force tests were made to determine the static longitudinal and lateral stability and control characteristics of the model for use in correlation with the flight-test results. In the power-off tests, the propeller was allowed to windmill. In the power-on longitudinal tests, an effort was made in some cases to simulate steady level flight by trimming the model in both pitch and drag. Once the thrust setting of the motor was determined for these conditions, it was then held constant over the remainder of the angle-of-attack range.

Most of the force tests were made over an angle-of-attack range of the platform from -10° to 20° for wing incidences of 20°, 25°, and 30°. (The angle-of-attack range of the keel covered by this group of tests varied from 10° to 50°.) Most of the lateral tests were made for sideslip angles of $\pm 5^{\circ}$ although a few tests were made over an angle-of-sideslip range from -20° to 20°. The tests to determine the lateral control effectiveness of the wing were made for wing-bank angles of $\pm 5^{\circ}$ and $\pm 10^{\circ}$ and wing-tip deflection angles of $\pm 5^{\circ}$, $\pm 10^{\circ}$, and $\pm 15^{\circ}$. Tests to determine the effectiveness of the vee-tail control surfaces were made for deflections of $\pm 10^{\circ}$ and $\pm 20^{\circ}$ for both elevator and rudder control. For the horizontal-tail and rudder arrangement mounted in the slipstream, control deflections were $\pm 10^{\circ}$ and $\pm 20^{\circ}$ for elevator control and $\pm 10^{\circ}$ for rudder control.

All the tests were run at a dynamic pressure of about 1.00 pound per square foot which corresponds to an airspeed of about 30 feet per second at standard sea-level conditions and to a test Reynolds number of about 1,660,000 based on the parawing keel length of 8.67 feet.

RESULTS AND DISCUSSION

Force Tests

Static longitudinal stability and control characteristics.- The results of force tests to determine the static longitudinal stability and control characteristics of the model are presented in figure 5 for wing incidences of 20°, 25°, and 30°. These data show that the effects of power on the longitudinal characteristics of the model are relatively small except for the $i_w = 30°$ condition. For this condition, power delayed the stall and increased the maximum lift coefficient.

In order to permit a comparison of the effects of wing incidence on the longitudinal characteristics more conveniently, the data of figure 5 for i_w conditions of 20°, 25°, and 30° are replotted in figure 6(a) for the power-off case. Also presented in figure 6(a) are data for the model with the parawing off. (For comparison, the data are referred to the keel angle in fig. 6(b).) The data for the complete configuration show that increasing the angle of incidence of the parawing increased the lift coefficient at which pitch trim occurred and reduced the static longitudinal stability (a result expected since an increase in wing incidence corresponds to a rearward shift in the center of gravity relative to the wing). At angles of attack near the stall, the pitching moments show a destabilizing break and then, at the stall, an abrupt nose-down or stabilizing break. The maximum value of $(L/D)_{trim}$ was about 4.2 and was obtained for the $i_w = 25°$ condition at a lift coefficient of about 0.75. The data for the model with the parawing off in figure 6(a) show relatively small values of lift, drag, and pitching moment.

The results of tests to measure the longitudinal characteristics of the model with the vee-tail off are presented in figure 7. Comparison of these results with those of the complete model of figures 5 and 6 shows in general that the vee-tail had little effect on the lift, drag, and pitching-moment characteristics. For ease of comparison, the pitching-moment data of figures 5, 6, and 7 are replotted in figure 8. The data of figure 8 show that the greatest effect of the vee-tail occurred at high angles of attack for the $i_w = 30°$ condition where it is seen that the addition of the tail resulted in erratic pitching-moment behavior. The use of power eliminated this erratic behavior and provided a stabilizing influence to the model.

Presented in figure 9 are the results of tests to determine the pitch effectiveness of the vee-tail configuration. The results of tests with power off (fig. 9(a)) and with power on (fig. 9(b)) show that the elevator was relatively weak in terms of control power and that, as might be expected, the effectiveness was not greatly different with power off or on.

Because of the relatively weak pitch control effectiveness of the basic vee-tail arrangement, several different tail modifications were investigated on the model, and, in addition, the use of wing-tip deflection for pitch control was investigated in an attempt to arrive at a more effective pitch control system. The results of tests to evaluate the pitch effectiveness of the various

control systems are presented in figures 10 to 13. Presented in figure 10 are data for the model with the basic vee-tail configuration modified to include a center horizontal panel. (See fig. 2(a).) This center panel was hinged to deflect directly with the vee-tail elevators for pitch control. A comparison of the data of figures 9 and 10 indicates that the addition of the center panel increased the pitch effectiveness of the model, particularly in the power-on case where the effectiveness of the basic vee-tail was approximately doubled by this modification.

Presented in figure 11(a) are longitudinal stability data for the model with a conventional horizontal tail mounted in the propeller slipstream. (This horizontal tail was formed by placing the two vee-tail panels together as illustrated in fig. 2(b).) For the power-on condition, the pitch effectiveness of the conventional horizontal tail is seen to be substantially greater than that for the basic vee-tail arrangement of figure 9. For the power-off condition, there is little difference in the effectiveness of the two arrangements. Although locating the horizontal tail in the propeller slipstream offers a means of obtaining large increases in control effectiveness, it has the disadvantage of possible large trim changes between the power-off and power-on conditions. Some information related to this problem was obtained in the present investigation (presented in fig. 11(b)) by measuring the power-off and power-on pitching moments of the model with the horizontal tail set at various angles of incidences and with the horizontal tail off. The data of figure 11(b) indicate that by careful alinement of the horizontal tail with the propeller slipstream, it is possible to take advantage of the increased control effectiveness provided by the slipstream without the disadvantage of large trim changes associated with power failure. (For example, with a tail incidence of 10°, the model was trimmed in pitch at a lift coefficient near the maximum value of L/D and the effects of power were relatively small.) On the other hand, when the horizontal tail was deflected to other angles of incidence (for example, -5°), the data of figure 11(b) show that there was a change in pitch trim in the event of a power failure, but that this trim change was only of about the same magnitude as that experienced with the vee-tail with the center panel added (see fig. 10).

Summarized in figure 12 are plots of the incremental pitching-moment coefficient against elevator deflection and of the elevator effectiveness parameter $\Delta C_{m_{\delta_e}}$ against S_t/S for the tail arrangements investigated. The results of this figure show very readily the benefit in control effectiveness derived from the slipstream dynamic pressure. From the plot of $\Delta C_{m_{\delta_e}}$ against S_t/S, it is seen that the conventional horizontal tail with power on had about four times the effectiveness of the basic vee-tail.

The data of figure 13 indicate that the use of the wing tips for pitch control was relatively ineffective on the present model. It should be pointed out that the wing-tip length of the model was 14 percent of the leading-edge length and that an increase in tip length should increase the effectiveness of the wing-tip control almost in direct proportion to the increase in ratio of tip length to leading-edge length. However, the wing-tip hinge moment would be expected to increase in proportion to the square of the increase in the ratio

of tip length to leading-edge length and can become relatively large for this type of control system.

Static lateral stability characteristics.- Representative static lateral stability characteristics of the model measured over an angle-of-sideslip range from -20° to 20° are presented in figures 14 to 16. The data of figure 16 show that with the wing tips unlocked, the directional stability and the dihedral effect were slightly reduced from those with the tips locked. These effects can be explained as follows: When the model is sideslipped, a rolling moment is produced about the parawing roll axis (this rolling moment is equivalent to the wing-bank hinge moment in a vehicle of this type) because of the dihedral effect of the wing $\left(\Delta C_l = C_{l_\beta}\beta\right)$. When the tips are locked, this rolling moment is opposed by the roll cables which lock the wing in bank. When the tips are unlocked, however, the sideslip rolling moment of the wing is opposed by a rolling moment produced by the wing tips since the tips deflect to oppose wing bank in proportion to the gearing ratio between the wing and tips. It was observed that very little wing bank and wing-tip deflection occurred when the model was sideslipped, which indicates that the wing tips were effective in neutralizing the rolling moment (or hinge moment) due to sideslip of the wing about its roll axis. This result indicates that in a full-size man-carrying vehicle, the lateral stick forces produced by sideslip would be relatively small compared with those usually encountered in a vehicle of this type employing wing bank alone for lateral control. (For example, see ref. 2.)

In order to analyze the results of figure 16 correctly, it is necessary to consider the various factors contributing to the net forces and moments about the center of gravity for the model in a sideslipped attitude with the wing tips unlocked. These factors are shown in the following expressions:

$$C_Y = C_{Y_\beta}\beta + C_L \sin \phi + C_{Y_{\delta_{tip}}}\delta_{tip} \tag{1}$$

$$C_n = C_{n_\beta}\beta + \frac{x}{b}C_L \sin \phi + C_{n_{\delta_{tip}}}\delta_{tip} \tag{2}$$

$$C_l = C_{l_\beta}\beta + \frac{z}{b}C_L \sin \phi + C_{l_{\delta_{tip}}}\delta_{tip} \tag{3}$$

In the side-force expression, the term $C_L \sin \phi$ represents the lateral component of the lift vector when the wing is banked and the term $C_{Y_{\delta_{tip}}}\delta_{tip}$ represents the side force produced by tip deflection. These two terms are of about the same order of magnitude but are opposite in sign for the conditions under consideration. In expressions (2) and (3), the terms $\frac{x}{b}C_L \sin \phi$ and $\frac{z}{b}C_L \sin \phi$ represent the yawing moment and rolling moment, respectively, produced by the lateral component of the lift vector for a banked condition. These terms are opposed, respectively, by the yawing moment and rolling moment

produced by the tip deflection. Substituting measured data into expressions (1) to (3) gives results which are generally similar to those of figure 16 for the wing tips unlocked. More information concerning these factors will be presented subsequently in the discussion of the control characteristics of the model.

The static lateral stability parameters C_{Y_β}, C_{n_β}, and C_{l_β} determined from figures 14 and 15 at sideslip angles of $\pm 5^\circ$, as well as from other lateral tests made at $\pm 5^\circ$, are presented in figures 17 to 19. The data of figure 17 show that the model had positive dihedral effect $\left(-C_{l_\beta}\right)$ for the angle-of-attack range of this investigation and was statically directionally stable except at the higher angles of attack. The data of figure 17(d) show that increasing the angle of incidence lowered the platform angle at which the model became directionally unstable. (In all cases, this instability occurred at a keel angle of attack of about 35°.) The data of figure 18 show that the vee-tail generally increased the directional stability and positive dihedral effect of the model. For the wing-off condition, the directional stability and dihedral effect were relatively small over the test angle-of-attack range. The data of figure 19 show that the addition of the rudder surface to the model provided a positive increment of C_{n_β} at low and high angles of attack in the power-off case. In the power-on case, a positive increment of C_{n_β} was obtained with the use of this surface over the entire angle-of-attack range because of the favorable effect of the propeller slipstream.

Static lateral control characteristics.- The static incremental lateral control characteristics produced by banking the parawing with respect to the platform are presented in figure 20 for i_w conditions of 20°, 25°, and 30°, and these data are summarized in figure 21 for the power-off case. The data of figures 20 and 21 show that banking the wing produced favorable rolling moments but also gave fairly large values of adverse yawing moments at higher angles of attack. Power effects were found to be relatively small for the conditions investigated. These results are generally similar to those of previous parawing configurations which employed wing bank for lateral control. (For example, see refs. 1 and 2.)

Previous analysis of the lateral control characteristics produced by wing bank has indicated that the adverse yawing moment associated with this type of control system can be attributed to the fact that the lift vector of the wing acts behind the center of gravity and when the wing is banked the lateral component of the lift vector produces a yawing moment through the horizontal moment arm from this vector to the center of gravity. The investigation of reference 2 pointed out that in tunnel tests in which the platform of the model remained fixed and the wing was banked there was considerable difference in static control data depending upon the axis about which the wing was banked. For example, in earlier parawing utility vehicles, the wing was banked about an axis parallel to the keel; in the model of the present investigation, the wing was banked about an axis parallel to the platform. In comparing the static roll-control data for these two cases, it will be found that wing bank on vehicles about an axis parallel to the keel produces relatively small rolling moments but favorable yawing moments whereas wing bank about an axis parallel to the platform

produces relatively high rolling moments but adverse yawing moments. Reference 2 indicated that under actual flight conditions the overall control effectiveness should be about the same for the two cases inasmuch as the yawing moments produce sideslip of the airplane (either favorable or adverse), and this sideslip, acting through the effective-dihedral parameter C_{l_β}, produces rolling moments that tend to equalize the net rolling moment acting in the two cases. In reference 2 an expression for easily calculating the net rolling-moment coefficient (rolling moment for the case of zero yawing moment) for configurations employing the wing bank control system was derived. This expression

$$\Delta C_{l,\text{net}} = \frac{z}{b} C_L \sin \phi \left(1 + \frac{C_{l_\beta}}{C_{n_\beta}} \frac{1}{L/D}\right)$$

was used to calculate the net rolling-moment coefficient produced by 5° wing bank for the model of the present investigation and the results are presented in figure 22. The plot in the lower portion of figure 22 shows that the net rolling-moment coefficient of the model was considerably lower than the pure rolling-moment coefficient measured in the tests and that the control system became ineffective at the higher angles of attack. This abrupt loss in $\Delta C_{l,\text{net}}$ at the higher angles of attack results from the fact that the rolling effectiveness factor, shown at the top of figure 22, drops off abruptly - mainly because of the loss of directional stability shown in figure 17(b). The fact that the net rolling-moment coefficient diminishes rapidly at the higher angles of attack is in agreement with the results of references 1 and 2 where it was shown in both small-model and large-scale tests that the use of wing bank for lateral control was ineffective at high angles of attack in parawing configurations of the utility vehicle type.

Presented in figures 23(a) and 23(b) are the lateral control characteristics of the model provided by differential deflection of the wing tips with the wing fixed at zero bank-angle. The incremental moment coefficients produced by wing-tip differential deflection (presented in fig. 23(c)) show that the wing tips produced favorable roll and yaw when deflected for roll control. In order to compare the rolling effectiveness of the wing tips on the same basis as that of the wing-bank system, the data of figure 23(a) were used to estimate the rolling moment produced for the case of zero yawing moment. This estimate was made by first determining the equilibrium sideslip condition where $\beta = \Delta C_n / C_{n_\beta}$. From the value of β thus established, the incremental rolling-moment coefficient introduced through the effective-dihedral parameter C_{l_β} was then determined by $\Delta C_l = C_{l_\beta} \beta$. This value of ΔC_l was then added to that shown in figure 23(c) to obtain the net rolling-moment coefficient produced by wing-tip deflection, and the results of these calculations are presented in figure 24. The data of figure 24 show that the estimated values of net rolling moment are generally considerably higher than the measured values and a comparison of these data with those of figure 22 indicates that the wing tips were more effective for roll control than was the use of wing bank. For an accurate comparison of the rolling effectiveness, it is necessary, of course, to consider the hinge moments as well as the rolling moments involved in the two systems. For this reason, a plot of the net rolling-moment coefficient against

incremental hinge-moment coefficient for the two systems was made and is presented in figure 25. The hinge-moment-coefficient data for the wing-tip control were estimated for the wing-bank system by using figure 24 and knowing that the rolling moment about the pivot (which was obtained from wing-alone data) was equal to the hinge moment. The plot of figure 25 is identical in form to that presented in figure 35(a) of reference 2 and shows that the wing-tip control system provided a given rolling moment for a substantially lower hinge moment than that of the wing-bank system.

The results of tests to determine the lateral control effectiveness of the 35° vee-tail rudders are presented in figure 26(a). These data show that the effects of power were small and that deflection of the vee-tail surfaces for yaw control produced favorable yawing moments but was accompanied by large adverse rolling moments.

Presented in figure 26(b) are the results of tests to determine the lateral control effectiveness of a vertical rudder surface mounted directly in the slipstream. These data show that incremental yawing moments produced by the rudder were small in the power-off case, but, as would be expected, were relatively large for the power-on condition.

Flight Tests

The model behavior during flight was observed by the pitch pilot located at the side of the test section and by the roll-yaw pilot located at the rear of the test section. The results obtained in the flight tests were primarily in the form of qualitative ratings of flight behavior based on the opinions of these pilots. Motion-picture records obtained in the tests were used to verify and correlate the ratings for the different tests of the model, and some of this film has been prepared as a supplement (film serial L-836) to this report and is available on loan.

Longitudinal stability and control characteristics.- The dynamic longitudinal stability characteristics of the model were found to be satisfactory over the angle-of-attack range of this investigation (keel angles of 20° to 31°). The decrease in static longitudinal stability of the model as the trim lift coefficient increased (see fig. 6(b)) did not appear to be of great significance in the flight behavior of the model up through the maximum angle of attack flown. If flights had been made through the stall, however, the data of figure 6(b) indicate that a pitch-up tendency might have been encountered.

Deflecting the vee-tail surfaces for pitch control was found to provide unsatisfactorily weak dynamic longitudinal control characteristics even with control deflections as large as ±25°. For steady, relatively undisturbed conditions, the vee-tail provided sufficient control to keep the model flying but this control was considered to be unsatisfactory for overcoming large disturbances or for providing adequate maneuver capability.

Even though the design vee-tail arrangement was considered unsatisfactory for longitudinal control, it was felt that the use of some type of horizontal tail should provide a superior method of controlling a parawing vehicle of this

type as opposed to control by pitching the wing (which is, in effect, control by center-of-gravity shift) because of the inherently lower stick forces involved and the elimination of unsatisfactory control gradients and inertia feedback problems associated with the center-of-gravity-shift control system. For this reason, a limited number of flight tests were made to explore the use of other horizontal-tail arrangements for longitudinal control.

In view of the fact that previous investigations have shown that substantial gains in control effectiveness can be obtained with control surfaces mounted directly in the propeller slipstream (see ref. 1), a few flights were made in which a movable horizontal surface was mounted directly behind the propeller disk. This surface, which was identical in size to the rudder surface mounted behind the propeller disk shown in figure 2(b), proved to be too small for adequate control power in pitch but showed enough promise as a longitudinal control device to warrant further studies with larger surfaces of this type. An example of such an arrangement is the horizontal tail formed by placing the two vee-tail panels together as illustrated in figure 2(b). This tail arrangement was not flight tested, but on the basis of the static control data of figure 12, it appears to offer a means of utilizing the existing vee-tail panels to obtain large increases in the longitudinal control power of the configuration.

Another longitudinal control system flight tested in the present investigation was that of wing-tip deflection for pitch control. This system was studied on the present model since in a preliminary flight investigation of a parawing configuration, it had shown some promise as a longitudinal control device. On the present model, however, this type of control was found to be relatively weak (as indicated by the control effectiveness data of fig. 13), apparently because of the small tip length involved. The response of the model in pitch to wing-tip deflection was generally similar to that of the model with the original vee-tail arrangement, particularly at the higher angles of attack; that is, the model could be flown satisfactorily under relatively undisturbed conditions but there was insufficient control for recovering the model from large disturbances or for providing adequate maneuver capability. In the lower angle-of-attack range, the control provided by the wing tips was somewhat improved, but the amount of control available was still considered inadequate.

One means of increasing the control effectiveness of the wing-tip control system would be to increase the wing-tip lengths. In fact, the control effectiveness probably would increase in direct proportion to the increase in tip length. It should be remembered, however, that the wing-tip hinge moments would be expected to increase in proportion to the square of the increase of the tip length and therefore careful consideration should be given to both of these factors in comparing the relative merits of this control system with those of other systems envisioned for controlling parawings in pitch.

Lateral stability and control characteristics.- The lateral stability characteristics of the model were found to be generally satisfactory over the angle-of-attack range. The model was directionally stable and the lateral oscillations were well damped.

The use of wing bank alone (no tip deflection) for lateral control generally provided a satisfactory means of controlling the model at the lower angles of attack of this investigation, but as the angle of attack increased there was a progressive deterioration in control effectiveness and at the higher angles of attack this control was considered ineffective for satisfactorily controlling the model. It was extremely difficult to keep the model under control and positioned in the test section in the high-angle-of-attack range; the slightest disturbance usually resulted in the model going out of control and diverging out of the test section. This loss in control effectiveness is generally similar to that experienced in previous flight-test investigations with parawing models of this type (see ref. 1) and is believed to be associated primarily with the relatively large adverse yawing moments generated with this type of control (see fig. 21) in combination with large values of positive effective dihedral and consequent reduction in net rolling-moment coefficient at high angles of attack (see fig. 22).

Flight tests of the model with combination wing-tip and wing-bank control (that is, with the wing tips geared to deflect much like a servo tab) indicated that the control effectiveness of the model was reduced somewhat compared with that experienced with wing bank alone. From overall considerations the control characteristics of this control system were probably generally similar to those with the wing tips fixed, but for any given angle of attack it appeared that the response of the model to control was more sluggish and sustained flights were even more difficult to achieve, particularly under disturbed conditions in the high angle-of-attack range. The reason for the reduced control effectiveness of this system is not completely understood, but it may be related to lag effects or to slight changes in the wing derivatives through tip deflection such as those indicated by the force-test data of figure 16. It should be pointed out that in a full-size man-carrying vehicle utilizing this type of lateral control, the reduction in stick forces achieved through the movable tips would probably more than mask the deteriorating effect of the geared tips on control effectiveness and the pilot would probably rate this combination control superior to the wing-bank-alone control. Both types of control would probably be unacceptable, however, on the basis of control power requirements of conventional airplanes.

Deflection of the vee-tail surfaces as rudders in combination with wing bank to reduce the adverse yawing due to wing bank resulted in a pilot-induced lateral oscillation which built up in amplitude because of control inputs as the pilot attempted to keep the model within the tunnel airstream. All flights with this arrangement were terminated by a control divergence. This divergence appeared to be caused by the reduction in roll control moments which resulted from the relatively large adverse rolling moment introduced when the vee-tail rudders were deflected for yaw control. (See fig. 26(a).) The vee-tail was therefore very unsatisfactory for lateral-directional control. Because of the unsatisfactory nature of the yaw control provided by the vee-tail surfaces, the vee-tail rudders were locked at neutral and a vertical rudder surface was installed on the model directly behind the pusher propeller to provide a source of favorable yawing moment. When this rudder was coordinated with the wing control, the model had satisfactory lateral control characteristics over the angle-of-attack range of this investigation. In fact, it appeared that the

model could be flown satisfactorily with the rudder alone at high angles of attack because of the high dihedral effect.

Another method of roll control which was investigated by flight tests was that of wing-tip deflection with the wing locked in bank. This system (developed and flight tested at Langley on the model of ref. 1) was found to be the most effective roll-control system investigated. The response of the model to control was rapid and very little attention was required by the roll-yaw pilot to maintain smooth sustained flights. In fact, because of the relatively high degree of rolling effectiveness, the model could be rolled to large angular displacements and then recovered easily by corrective control within the limited area of the tunnel test section. This rolling effectiveness was evidenced despite the relatively small tip length used on the present vehicle. The high rolling effectiveness in this case is apparently related to the fact that favorable yawing moments as well as favorable rolling moments were generated by wing-tip deflection. (See fig. 23(c).) Because of this favorable yawing moment with wing-tip deflection, it appeared that satisfactory lateral control could be provided with this system without the use of a rudder.

CONCLUDING REMARKS

The conclusions presented in the following sections were drawn from the results of the free-flight and force tests of a model of a parawing utility vehicle. The model was generally similar in design to an earlier model of a parawing utility vehicle flight tested, but incorporated several design changes, primarily in the area of control, which were intended to correct certain deficiencies of the earlier vehicle.

Stability

The model had satisfactory longitudinal and lateral stability over the angle-of-attack range covered in flight (keel angles of attack of 20° to 31°), but the force tests showed a pitch-up tendency and negative static directional stability at angles of attack above those covered in the flight tests.

Control

Design control system.- The control effectiveness provided by the design control system was unsatisfactory about each of the three axes in some flight conditions. The pitch control provided by the 35° vee-tail was much too weak for safe control of the model. When this vee-tail was used for yaw control, it produced such large adverse rolling moments that it was completely unsatisfactory as a yaw control. The wing-bank system used for roll control gave generally satisfactory control at low angles of attack. The control became progressively weaker with increasing angle of attack, however, and it was considered too weak for satisfactory control of the model at the higher angles of attack covered in the tests, either with the design condition in which the wing

tips were geared like servo tabs to reduce the wing hinge moments or when the wing tips were fixed.

Revised control system.- The force tests indicated that satisfactory longitudinal control could be provided by a horizontal tail the same size as the vee-tail located behind the propeller in the propeller slipstream. Satisfactory directional control was obtained in the flight tests with a rudder mounted in the propeller slipstream. Satisfactory roll control was obtained by the use of wing-tip deflection with the wing locked in bank. Because this type of roll control also provided favorable yawing moments, it appeared that satisfactory lateral control could be obtained by the use of wing-tip deflection without the use of a rudder.

Langley Research Center,
National Aeronautics and Space Administration,
Langley Station, Hampton, Va., September 30, 1964.

REFERENCES

1. Johnson, Joseph L., Jr.: Low-Speed Wind-Tunnel Investigation To Determine the Flight Characteristics of a Model of a Parawing Utility Vehicle. NASA TN D-1255, 1962.

2. Johnson, Joseph L., Jr.; and Hassell, James L., Jr.: Full-Scale Wind-Tunnel Investigation of a Flexible-Wing Manned Test Vehicle. NASA TN D-1946, 1963.

3. Paulson, John W.; and Shanks, Robert E.: Investigation of Low-Subsonic Flight Characteristics of a Model of a Hypersonic Boost-Glide Configuration Having a 78° Delta Wing. NASA TN D-894, 1961.

TABLE I.- MASS AND DIMENSIONAL CHARACTERISTICS OF THE MODEL

Weight, lb	78.0
Wing loading, lb/sq ft	1.47
Moment of inertia, slug-ft^2:	
I_X	14.6
I_Y	15.7
I_Z	11.7
Parawing dimensions:	
Area (developed, 45° leading-edge sweep), sq ft	53.15
Span (based on 45° leading-edge sweep condition), ft	12.26
Keel length, ft	8.67
Vee-tail dimensions:	
Area (two panels), sq ft	5.62
Span (projected), ft	5.4
Tip chord, ft	1.17
Root chord, ft	1.5
Rudder dimensions:	
Area, sq ft	1.50
Span, ft	2.0
Chord, ft	0.75

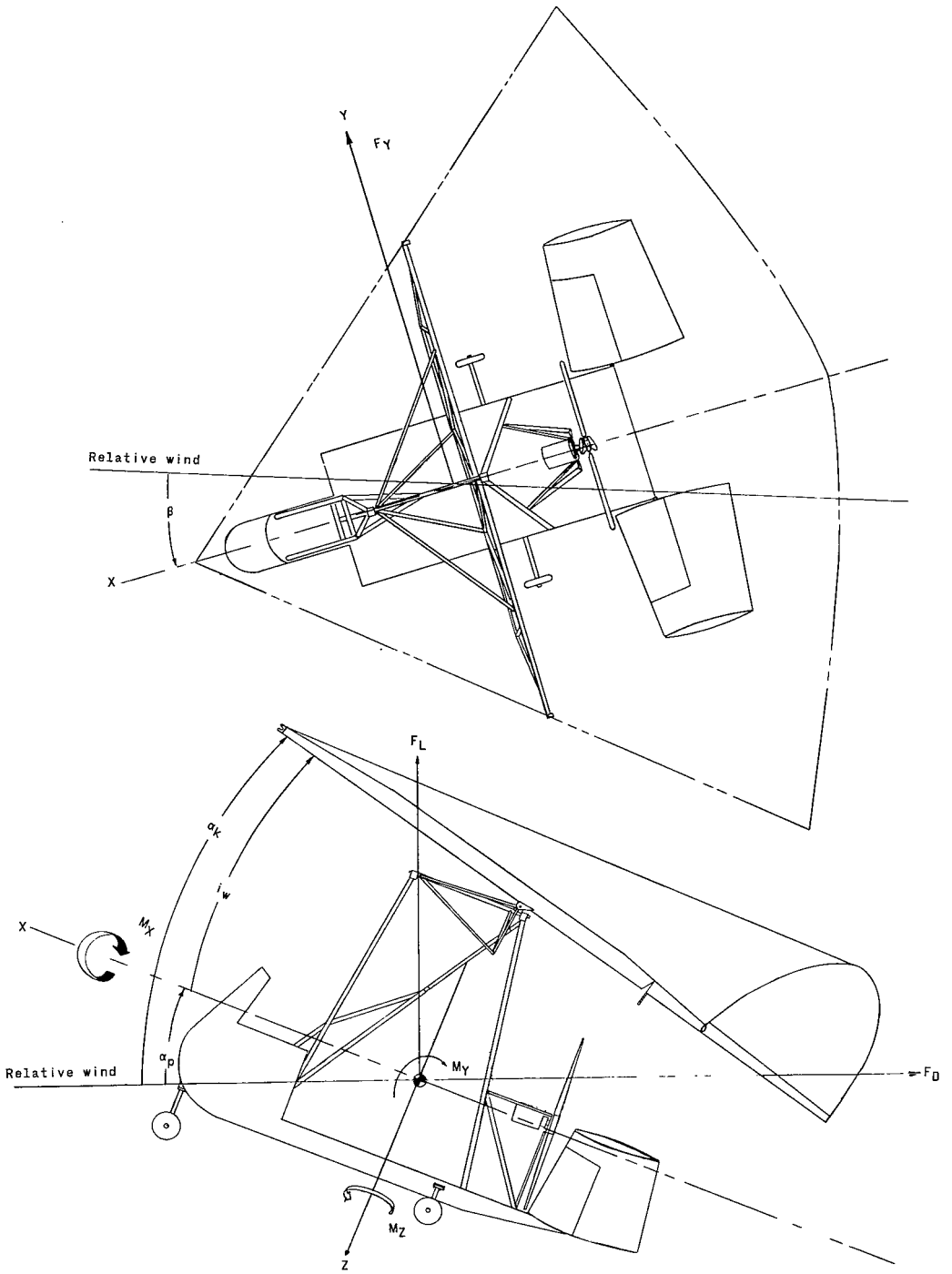

Figure 1.- System of axes used in investigation. Longitudinal data are referred to wind axes and lateral data are referred to body axes unless otherwise specified. Arrows indicate positive direction of moments, forces, and angles.

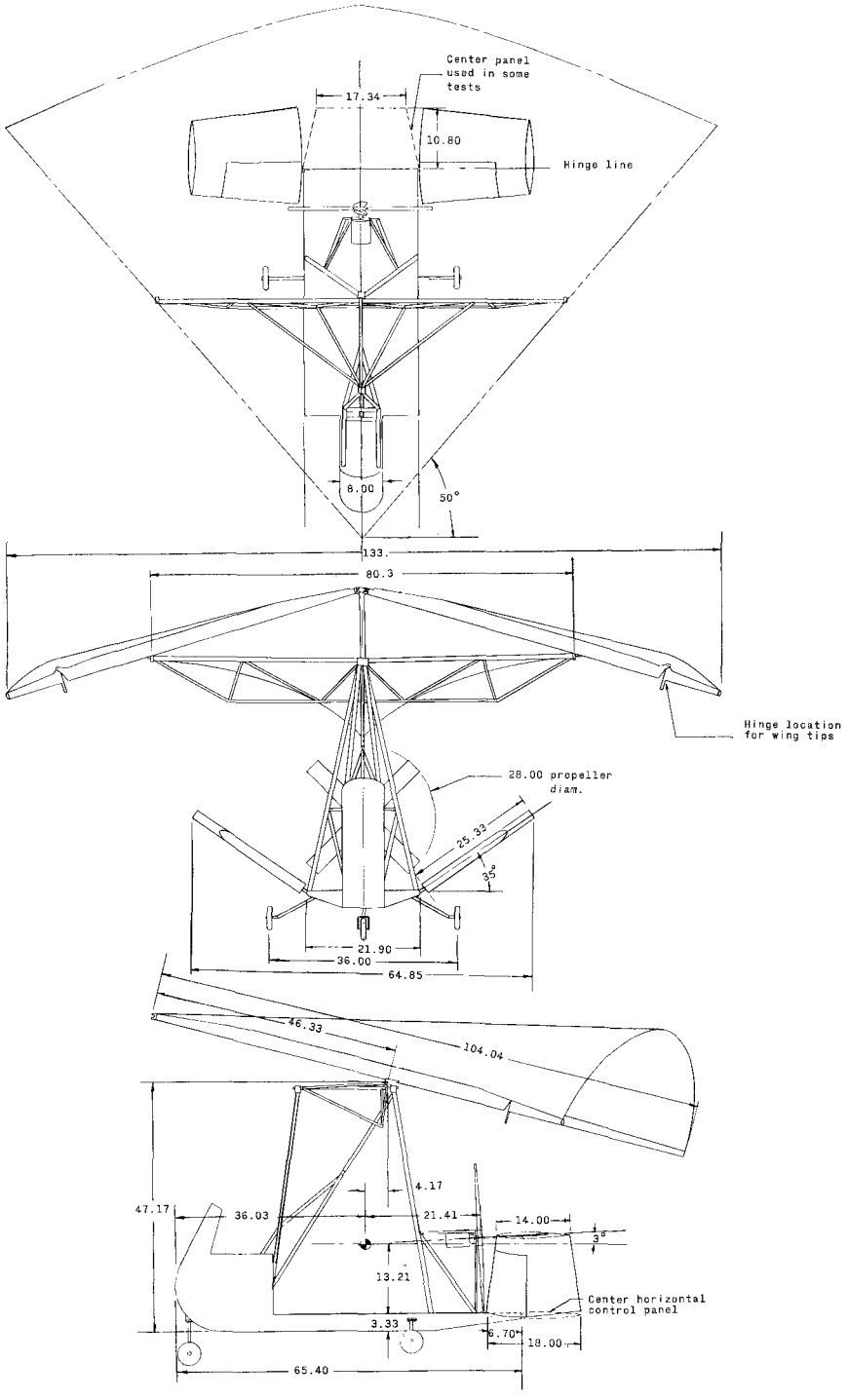

(a) Vee-tail arrangement.

Figure 2.- Three-view drawing of model used in investigation. All dimensions are in inches.

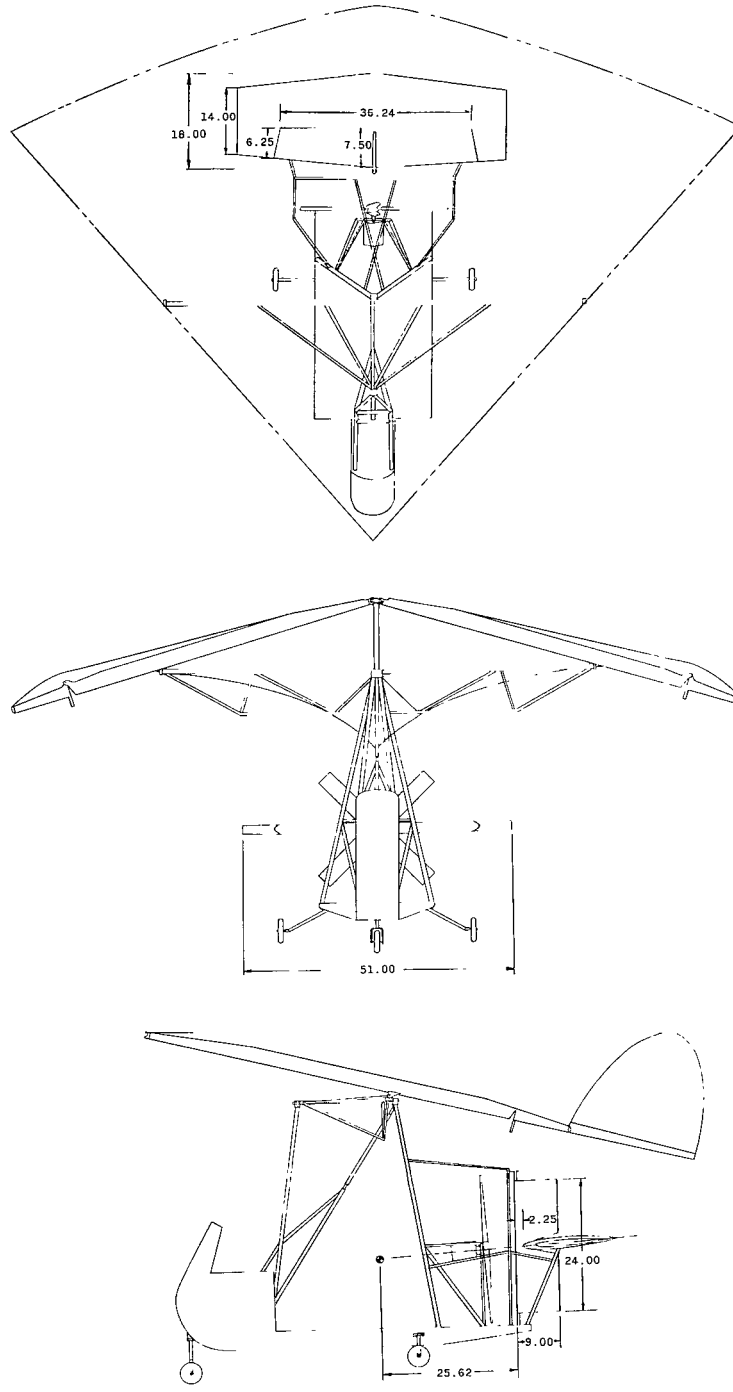

(b) Revised tail arrangement.

Figure 2.- Continued.

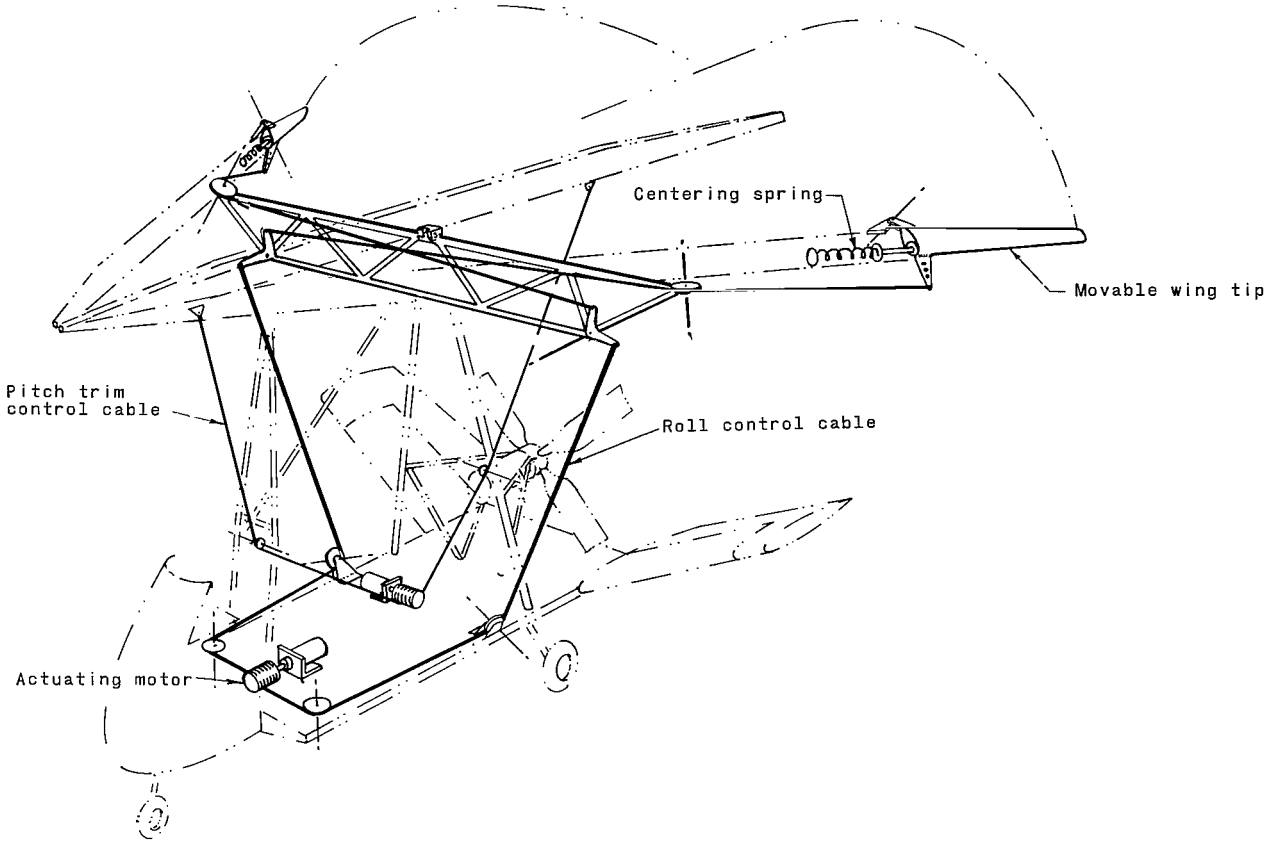

(c) Lateral control system and pitch trim system used on model.

Figure 2.- Concluded.

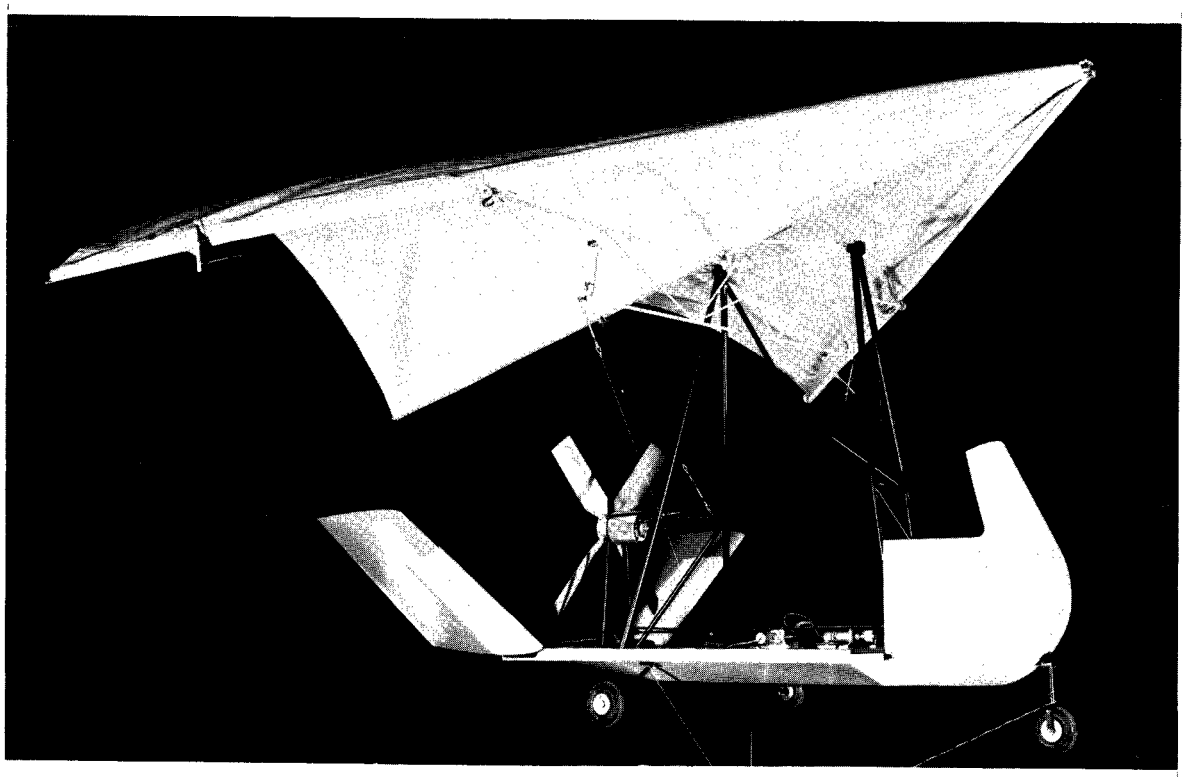

(a) Three-quarter front view of model. L-63-3249

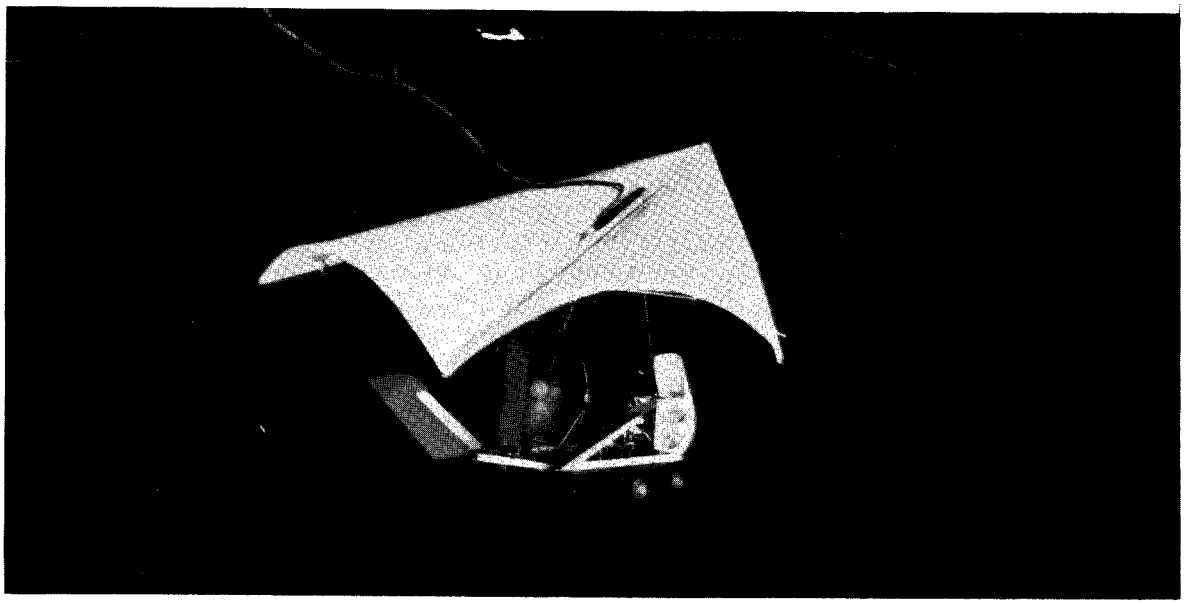

(b) Three-quarter rear view of model flying in Langley full-scale tunnel. L-63-3697

Figure 3.- Photographs of model.

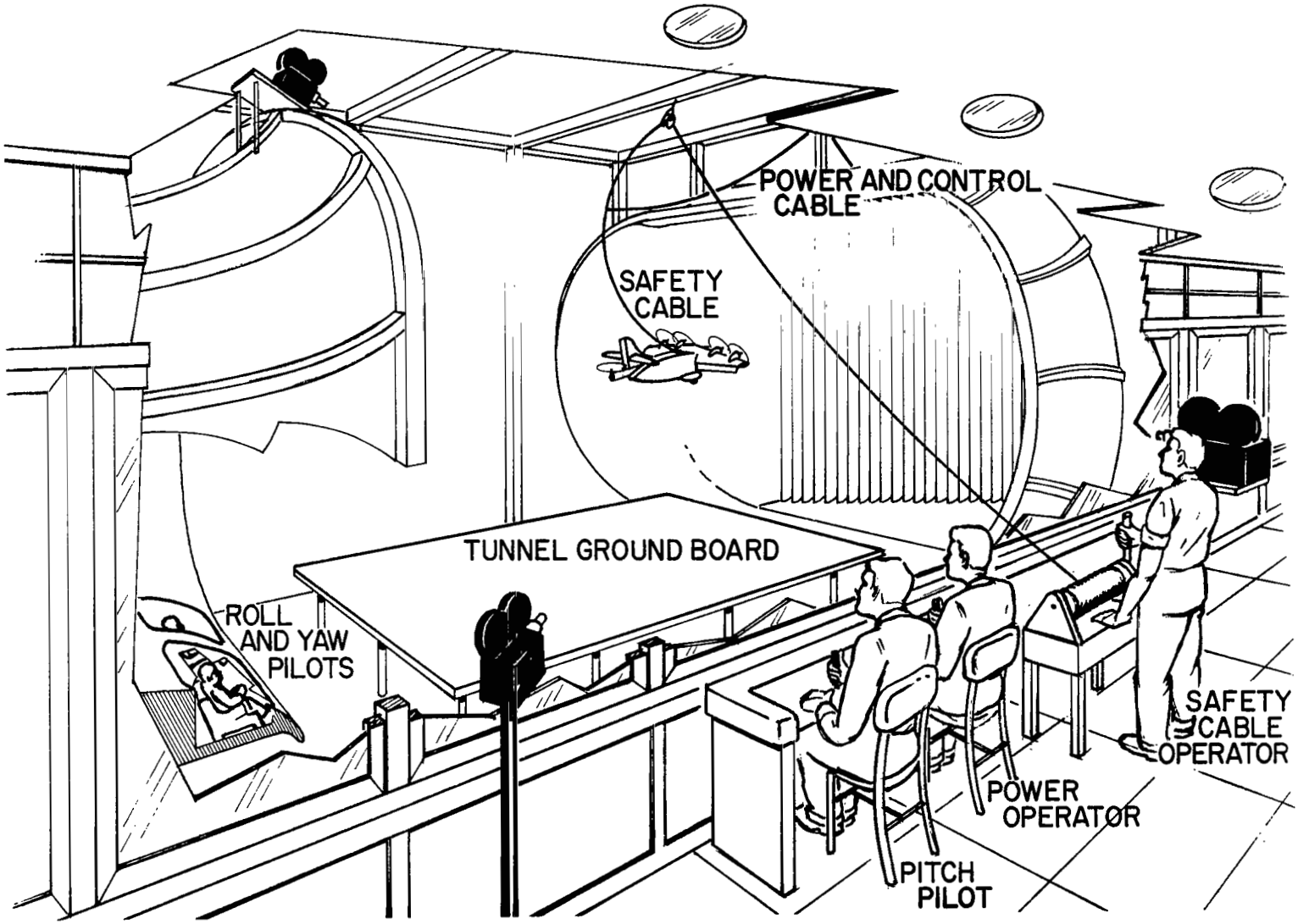

Figure 4.- Sketch of flight-test setup in Langley full-scale tunnel.

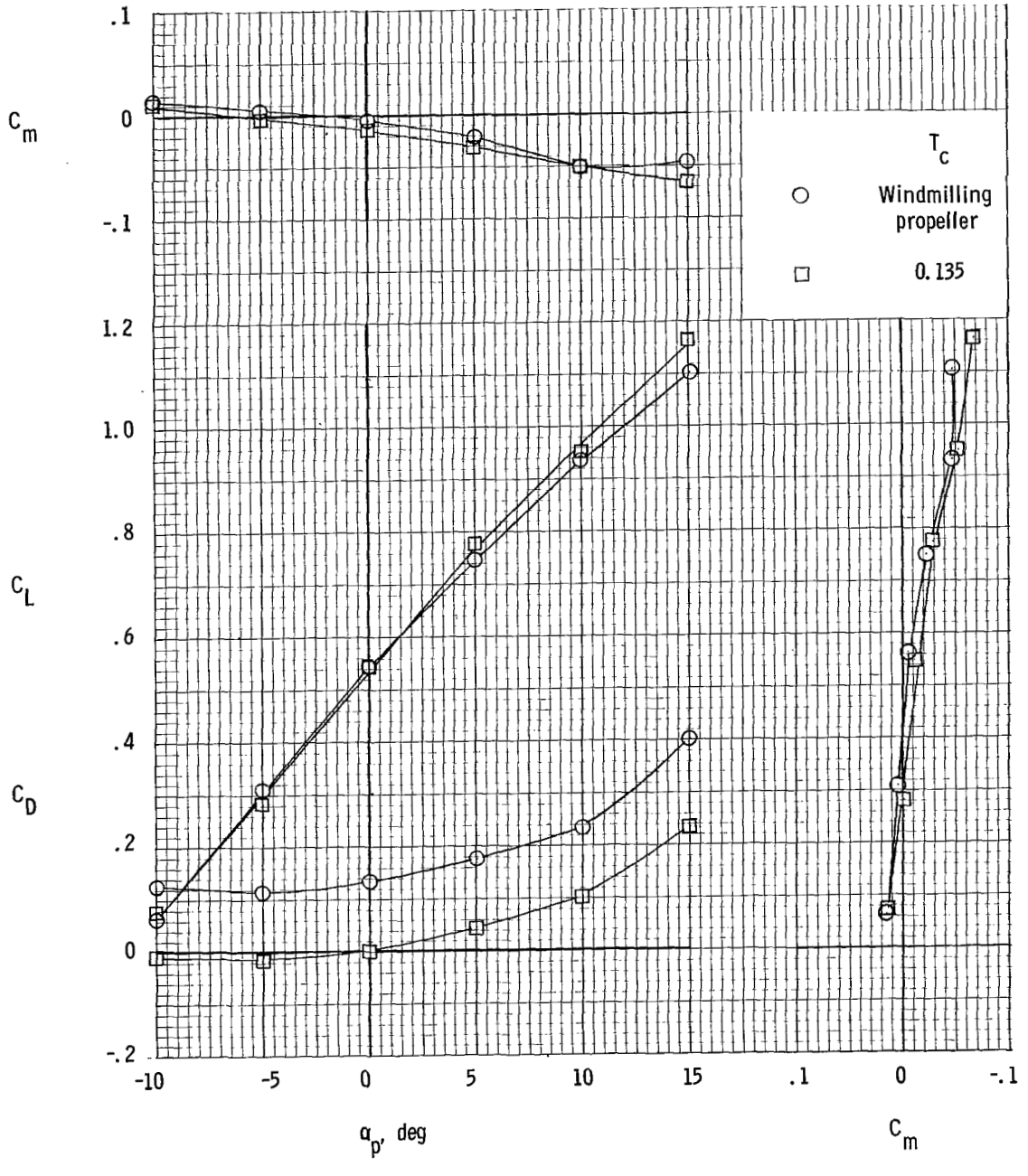

(a) $i_w = 20^\circ$.

Figure 5.- Static longitudinal characteristics of model. Design configuration; $\delta_e = 0^\circ$.

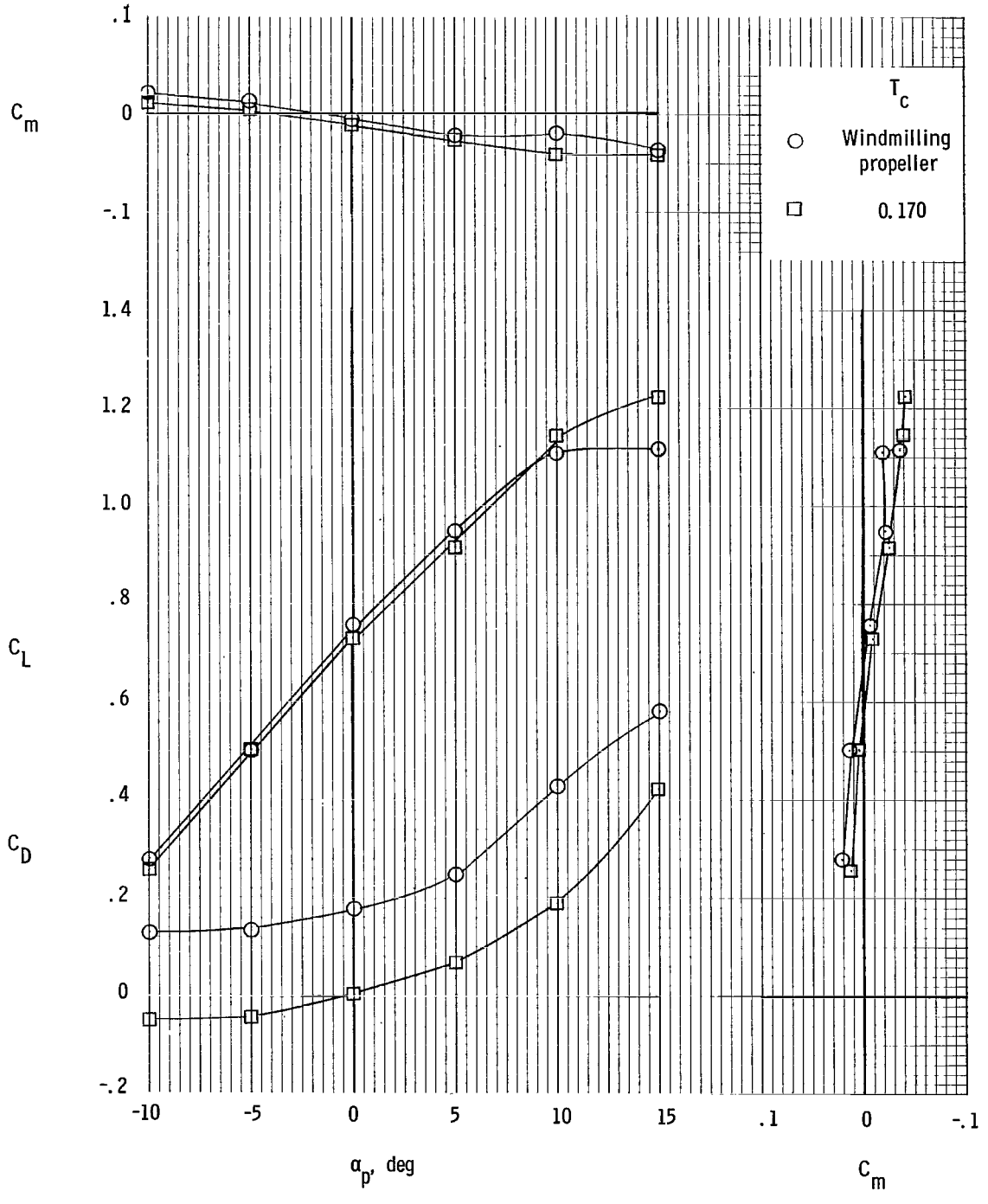

(b) $i_w = 25^\circ$.

Figure 5.- Continued.

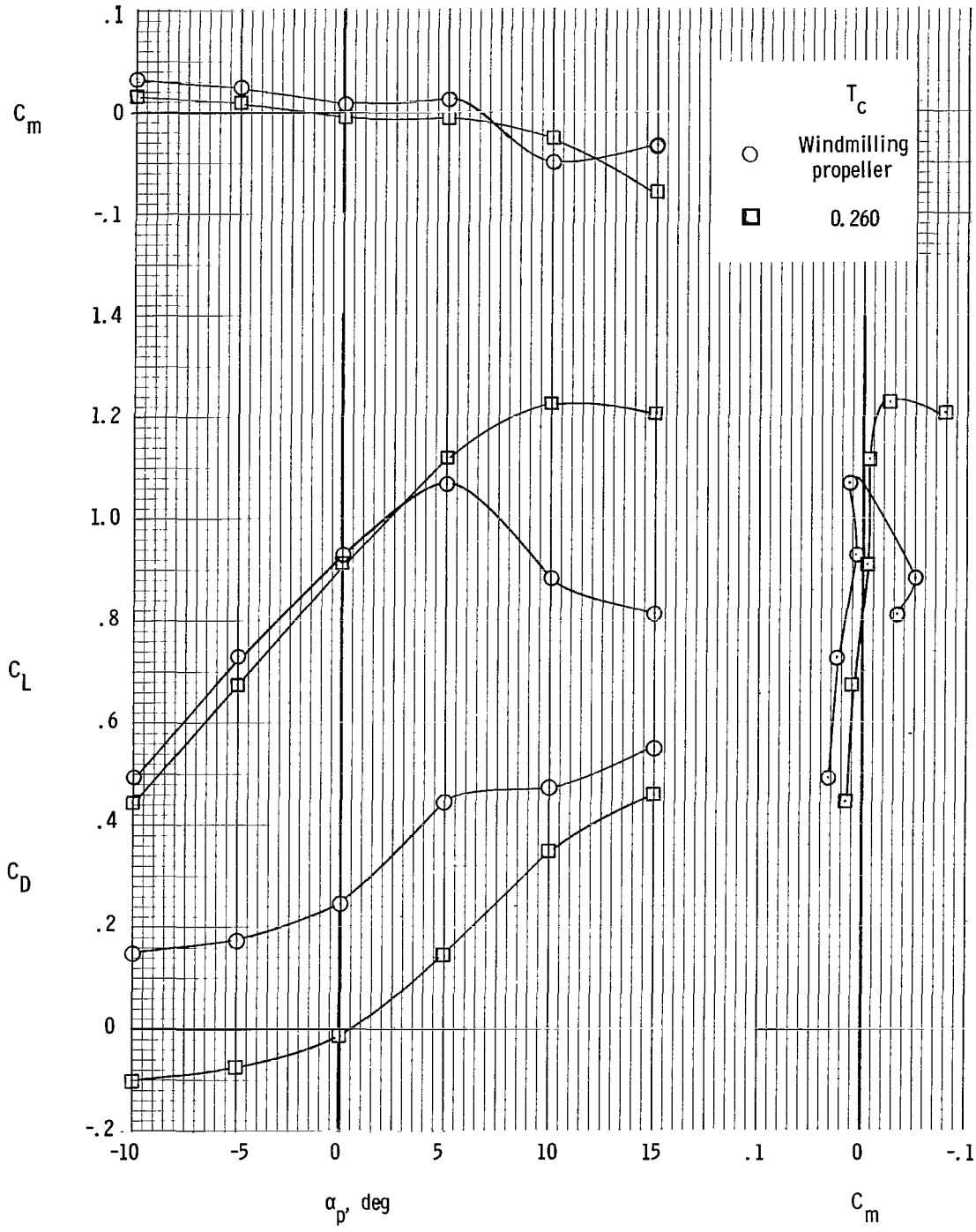

(c) $i_w = 30^\circ$.

Figure 5.- Concluded.

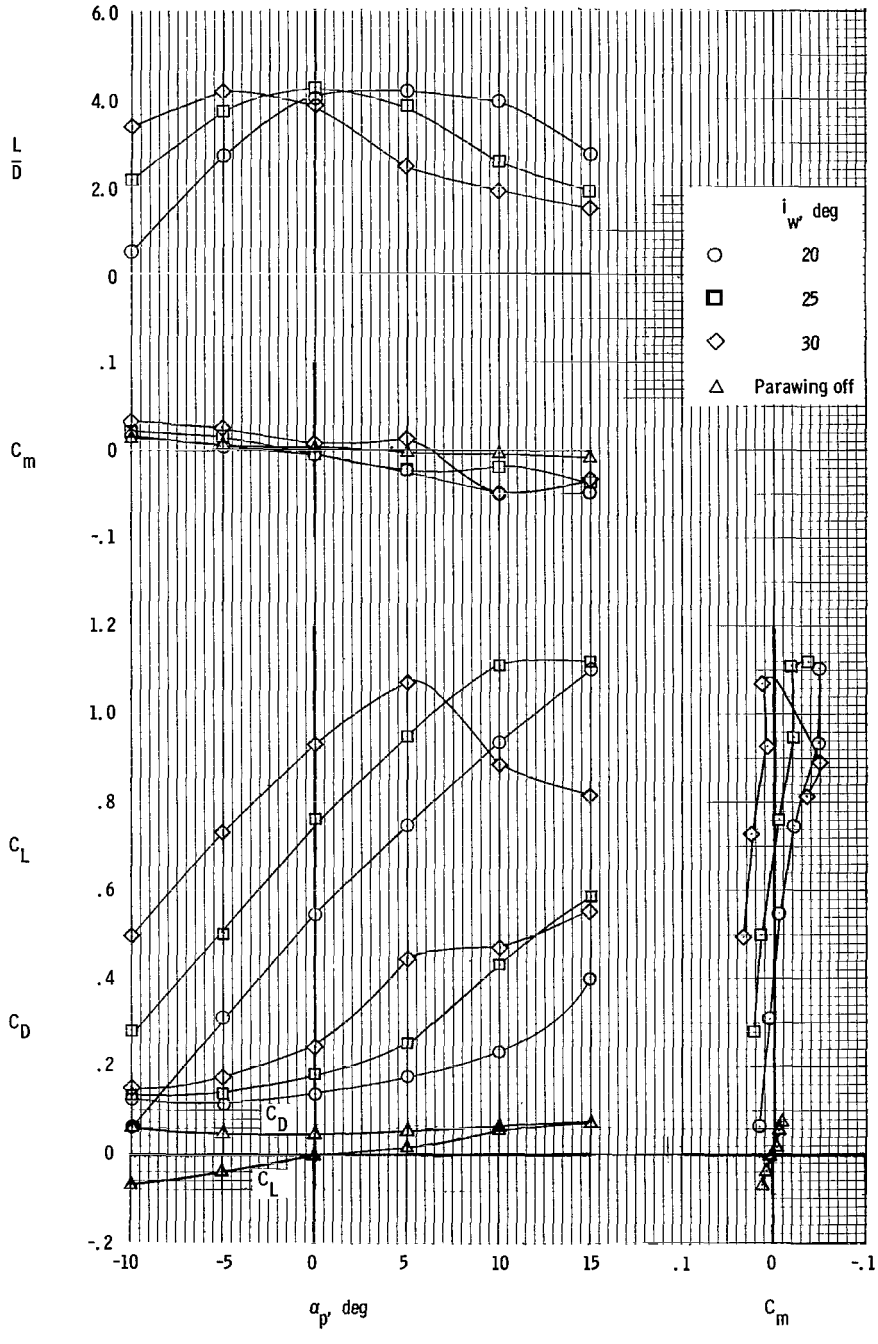

(a) Data plotted against platform angle.

Figure 6.- Summary of static longitudinal characteristics of model. Design configuration; windmilling propeller; $\delta_e = 0^o$.

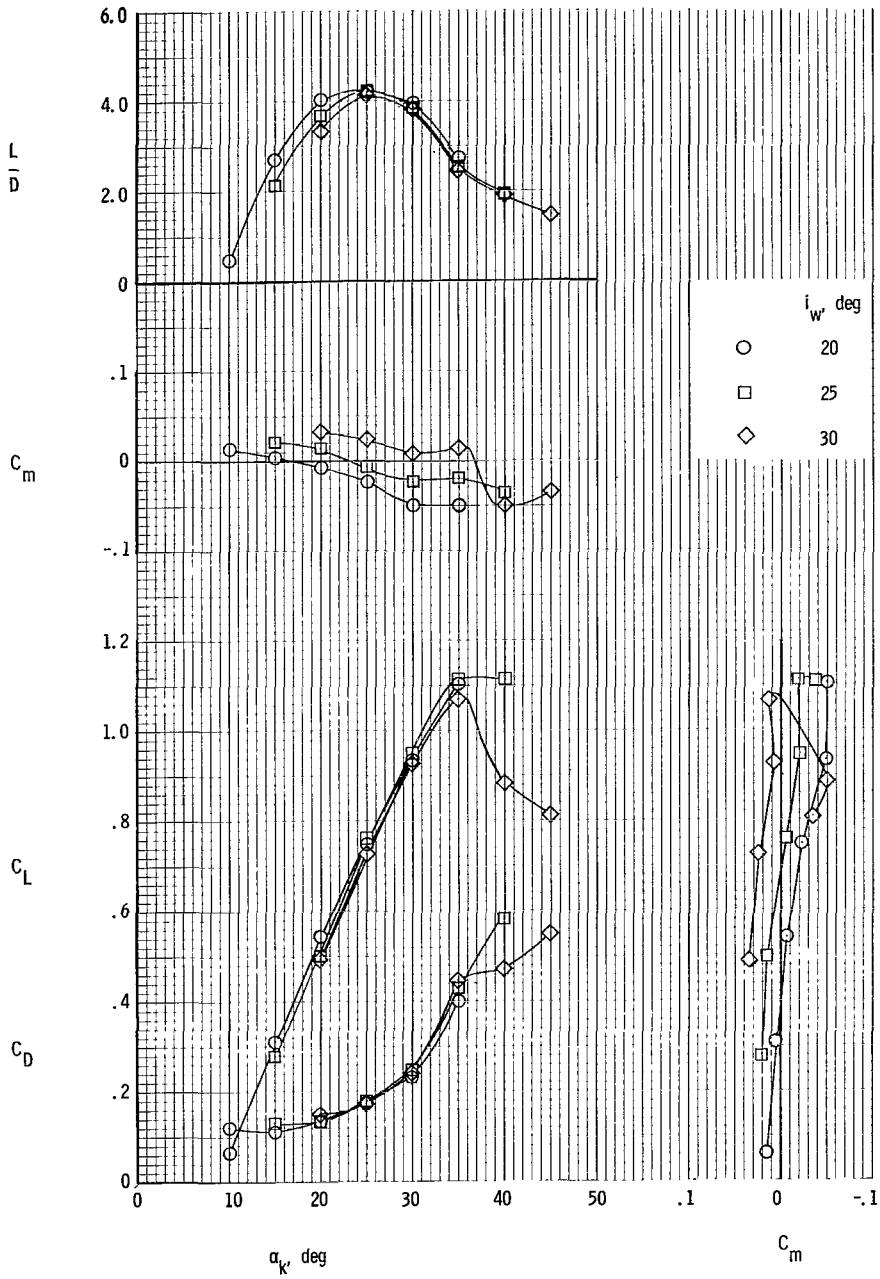

(b) Data plotted against keel angle.

Figure 6.- Concluded.

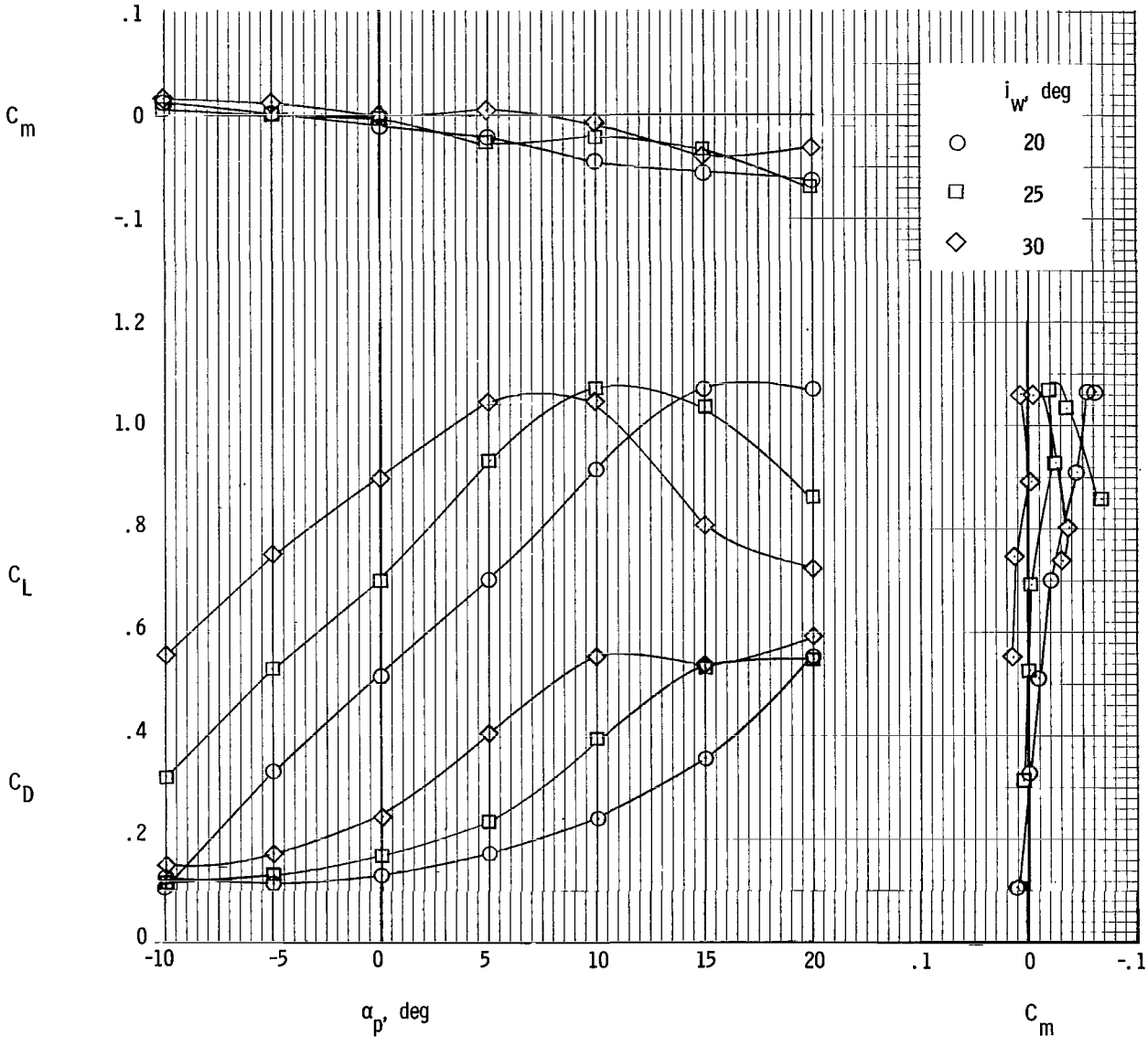

Figure 7.- Static longitudinal characteristics of model. Vee-tail off; windmilling propeller.

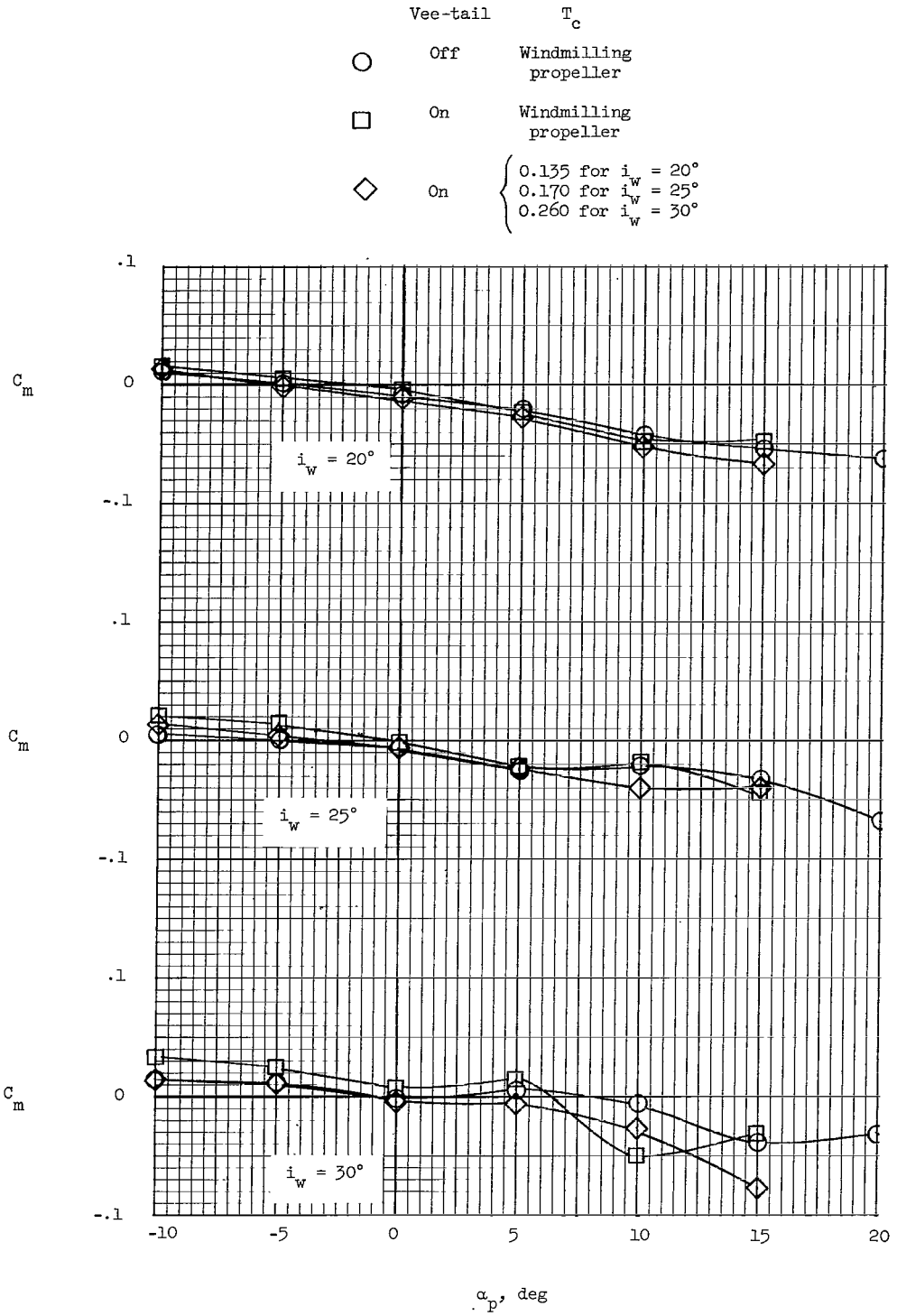

Figure 8.- Summary of pitching-moment characteristics of model.

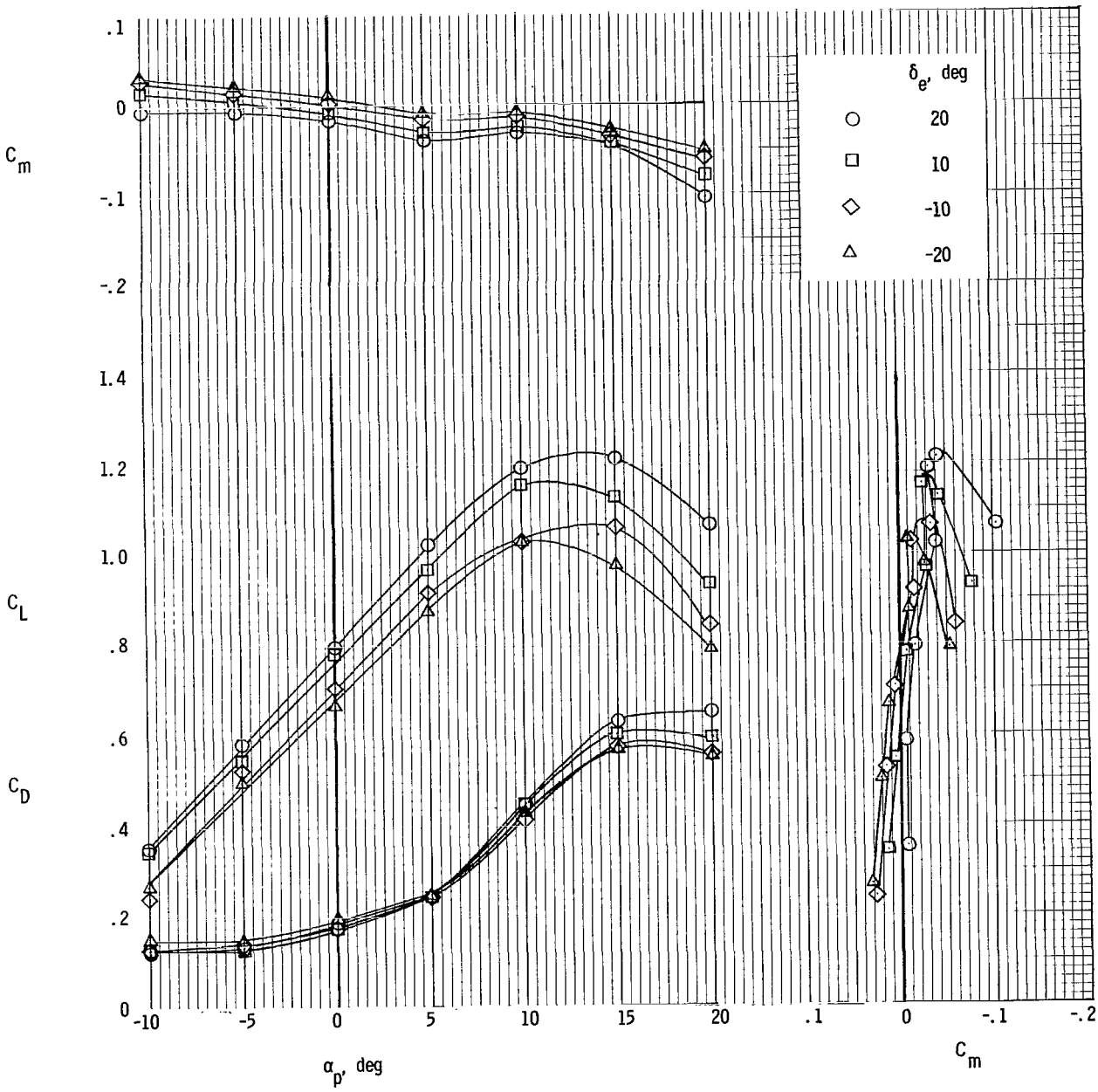

(a) Windmilling propeller.

Figure 9.- Pitch effectiveness of model with vee-tail configuration. $i_w = 25^\circ$.

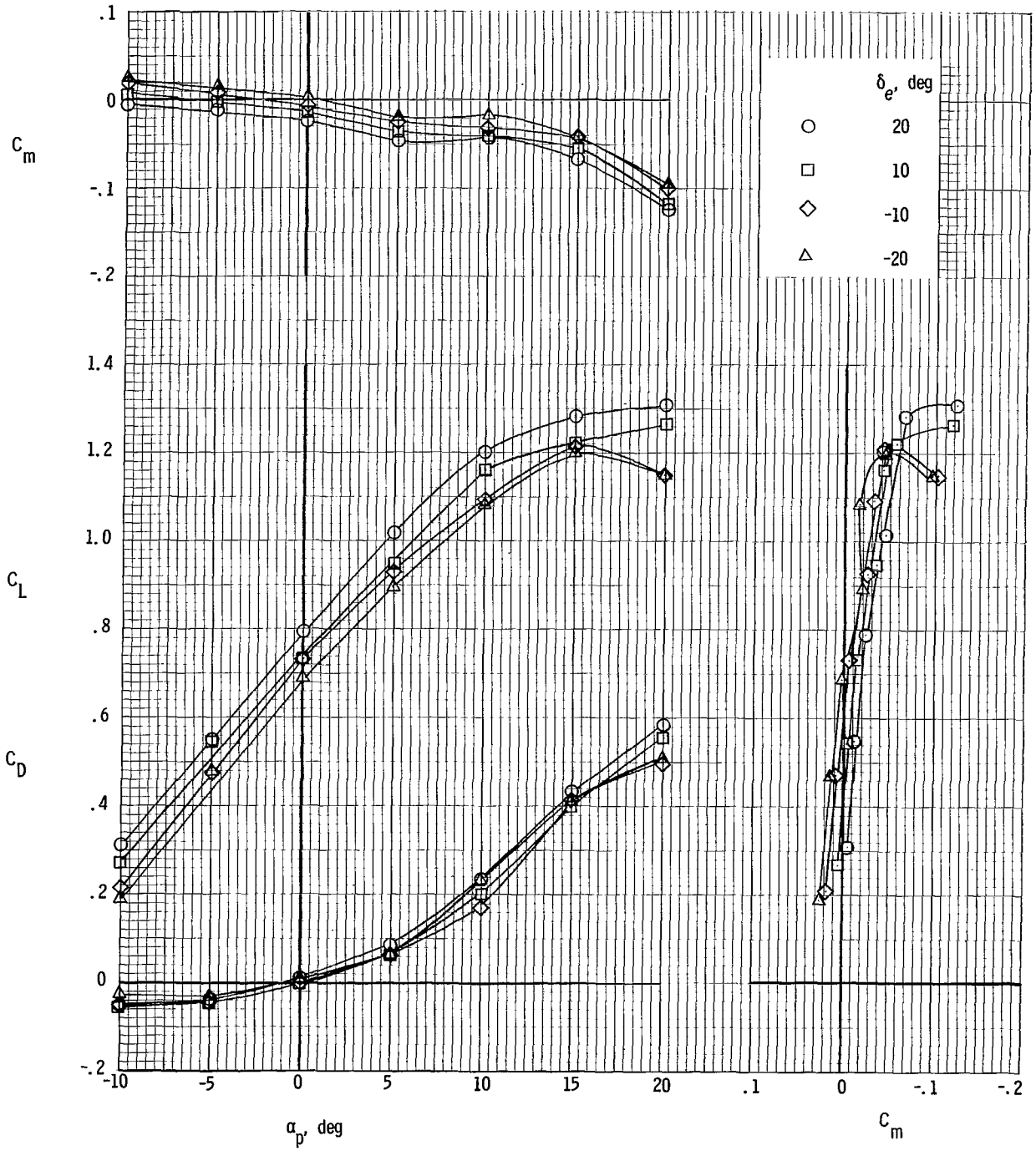

(b) $T_c = 0.170$.

Figure 9.- Concluded.

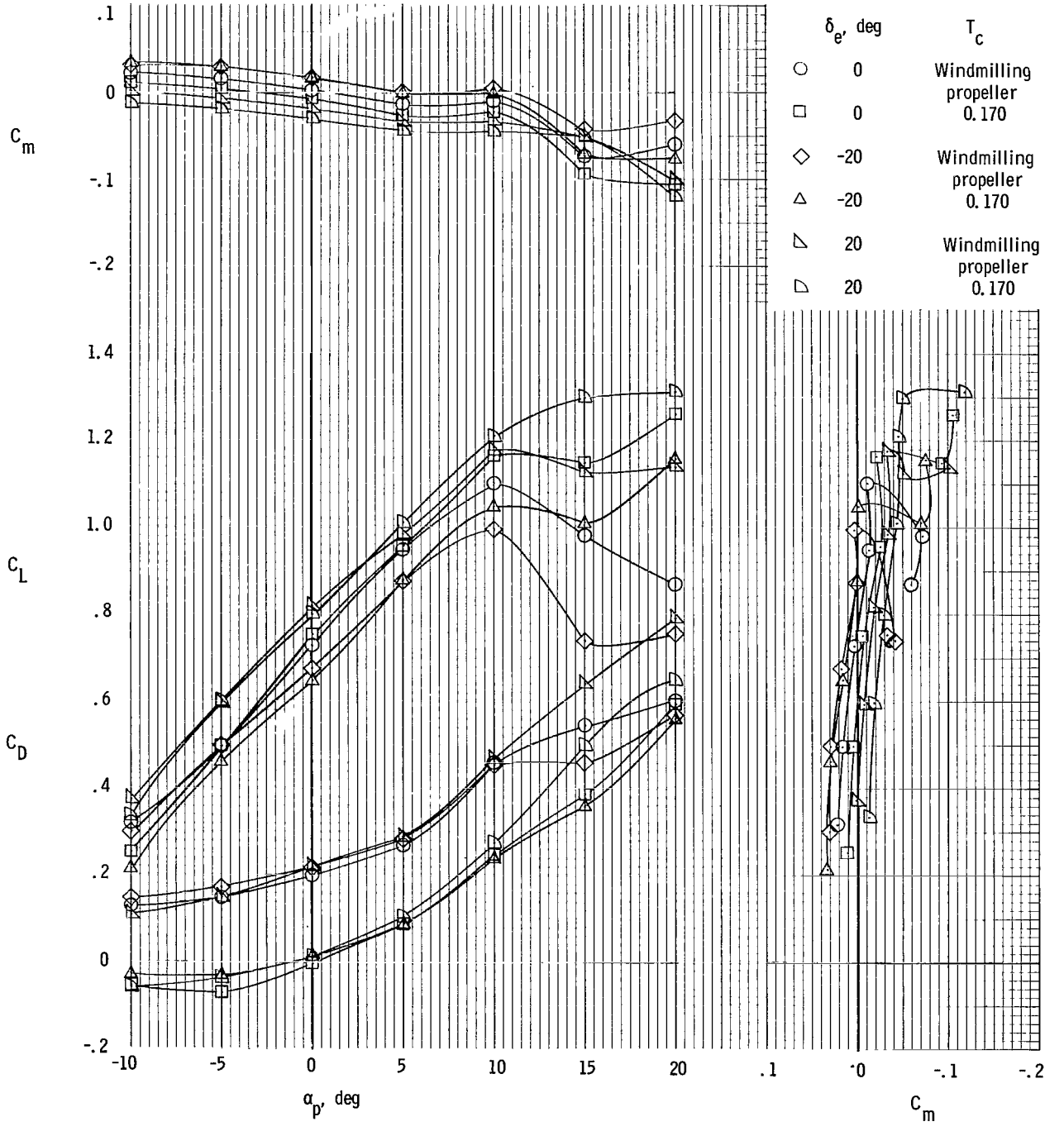

Figure 10.- Longitudinal characteristics of model with vee-tail configuration modified to include a center horizontal panel. $i_w = 25^\circ$.

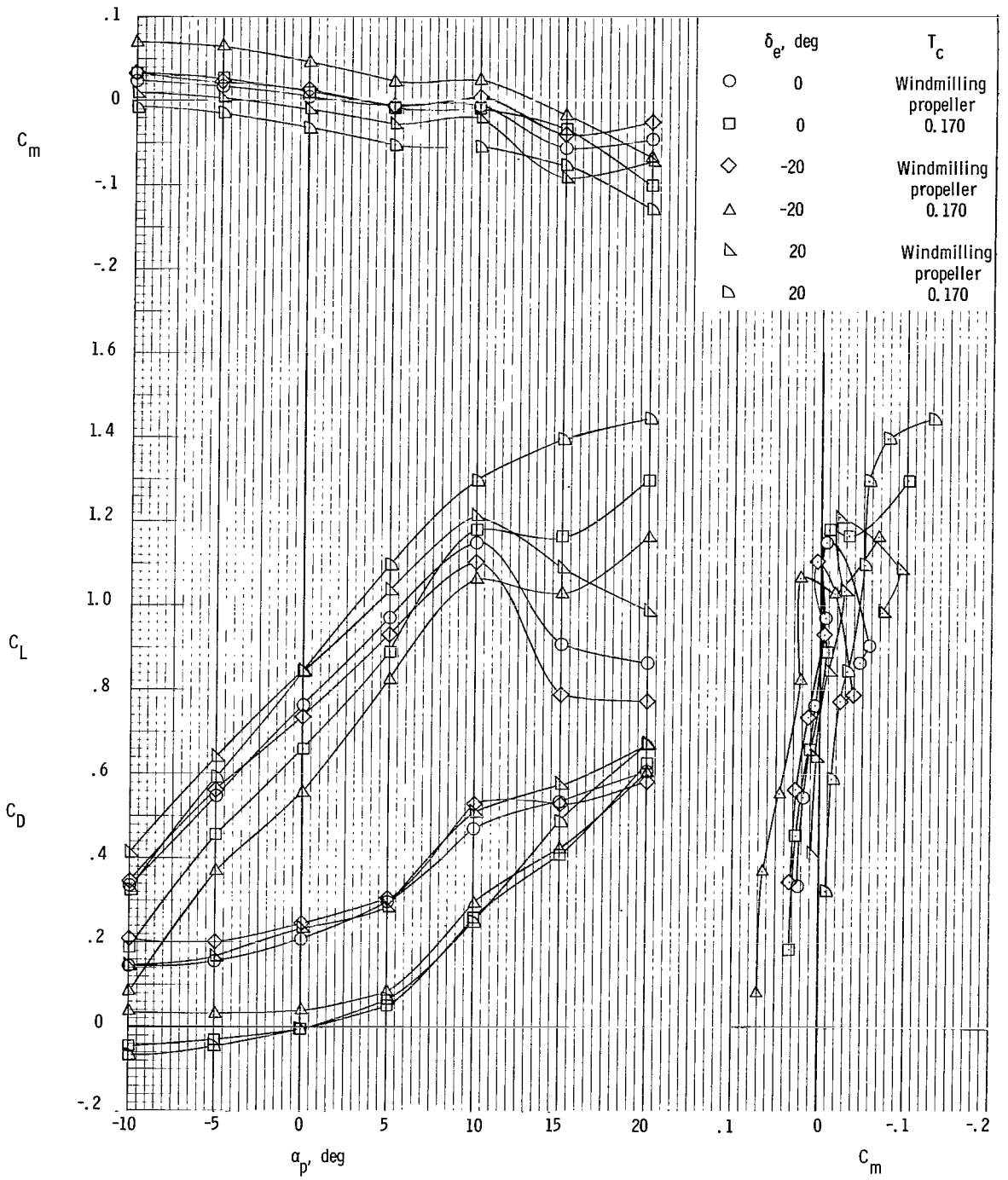

(a) Lift, drag, and pitching-moment characteristics.

Figure 11.- Pitch effectiveness of model with horizontal tail mounted in propeller slipstream. $i_w = 25^\circ$; $i_t = 0^\circ$.

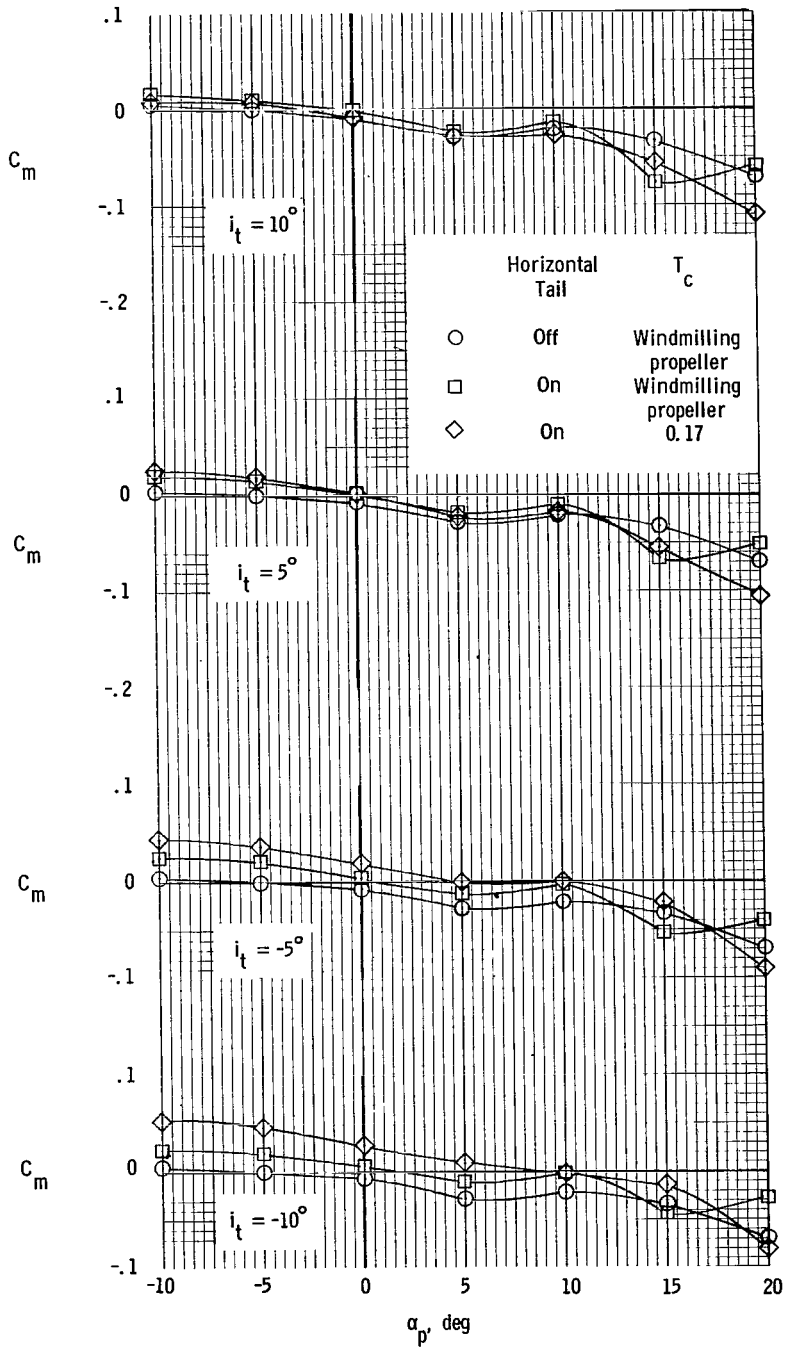

(b) Effect of horizontal-tail incidence on pitching-moment characteristics.

Figure 11.- Concluded.

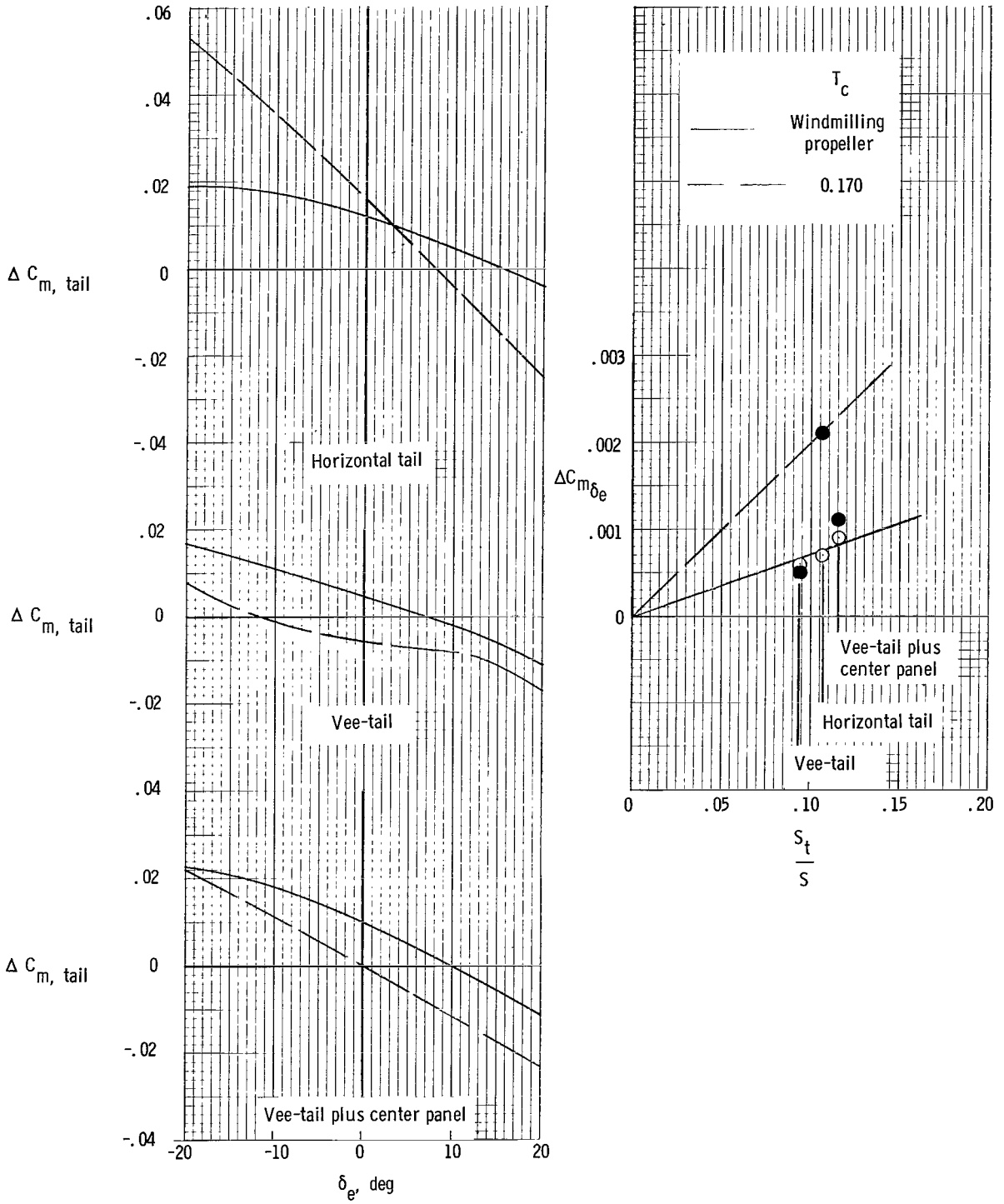

Figure 12.- Summary of pitching-moment effectiveness of model with various tail arrangements investigated. $i_w = 25^\circ$; $\alpha_p = 0^\circ$; $i_t = 0^\circ$.

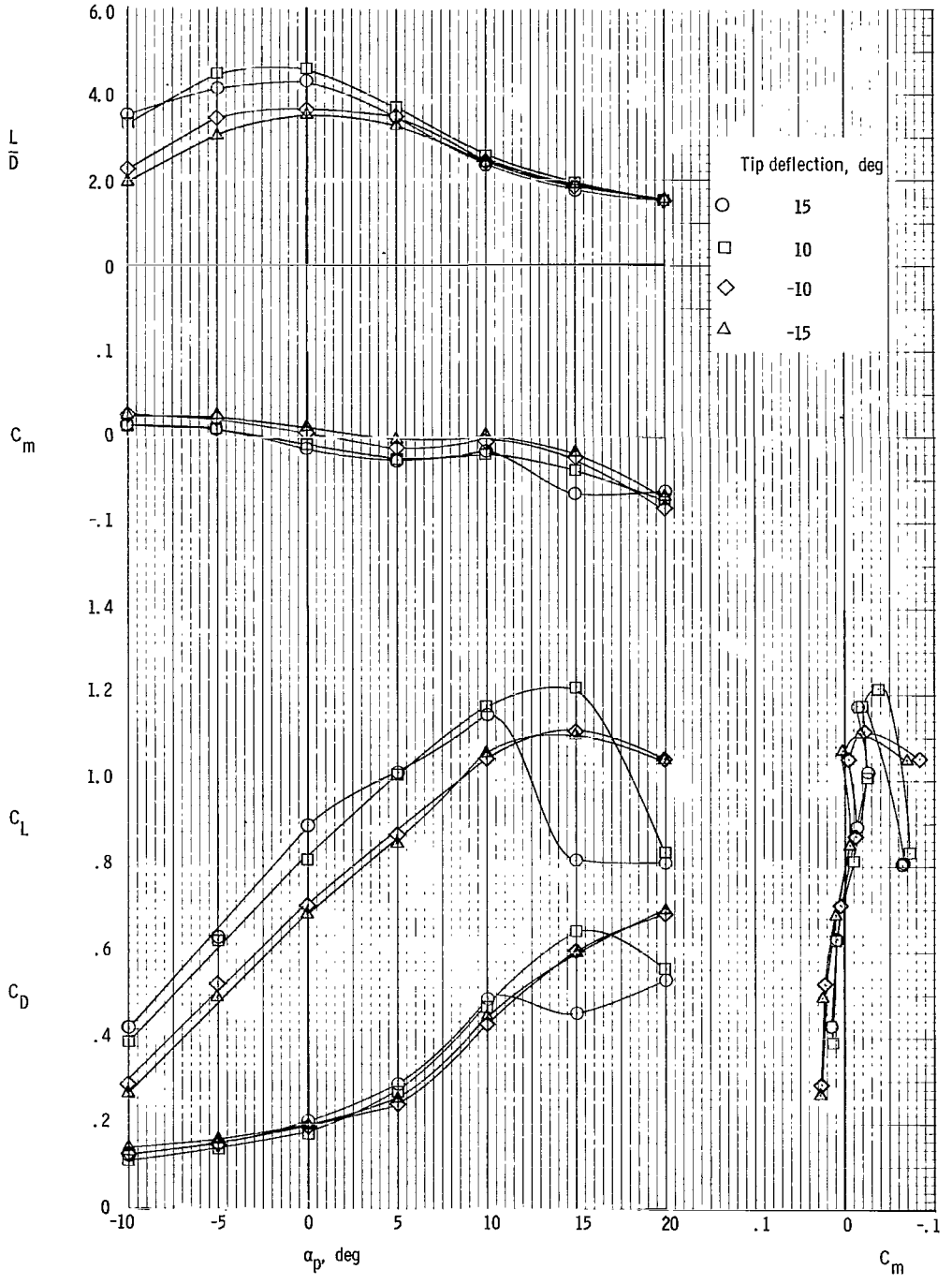

Figure 13.- Effect of symmetrical deflection of hinged wing tips for pitch control on longitudinal characteristics of model. Vee-tail on; windmilling propeller; $i_w = 25^\circ$; $\delta_e = 0^\circ$.

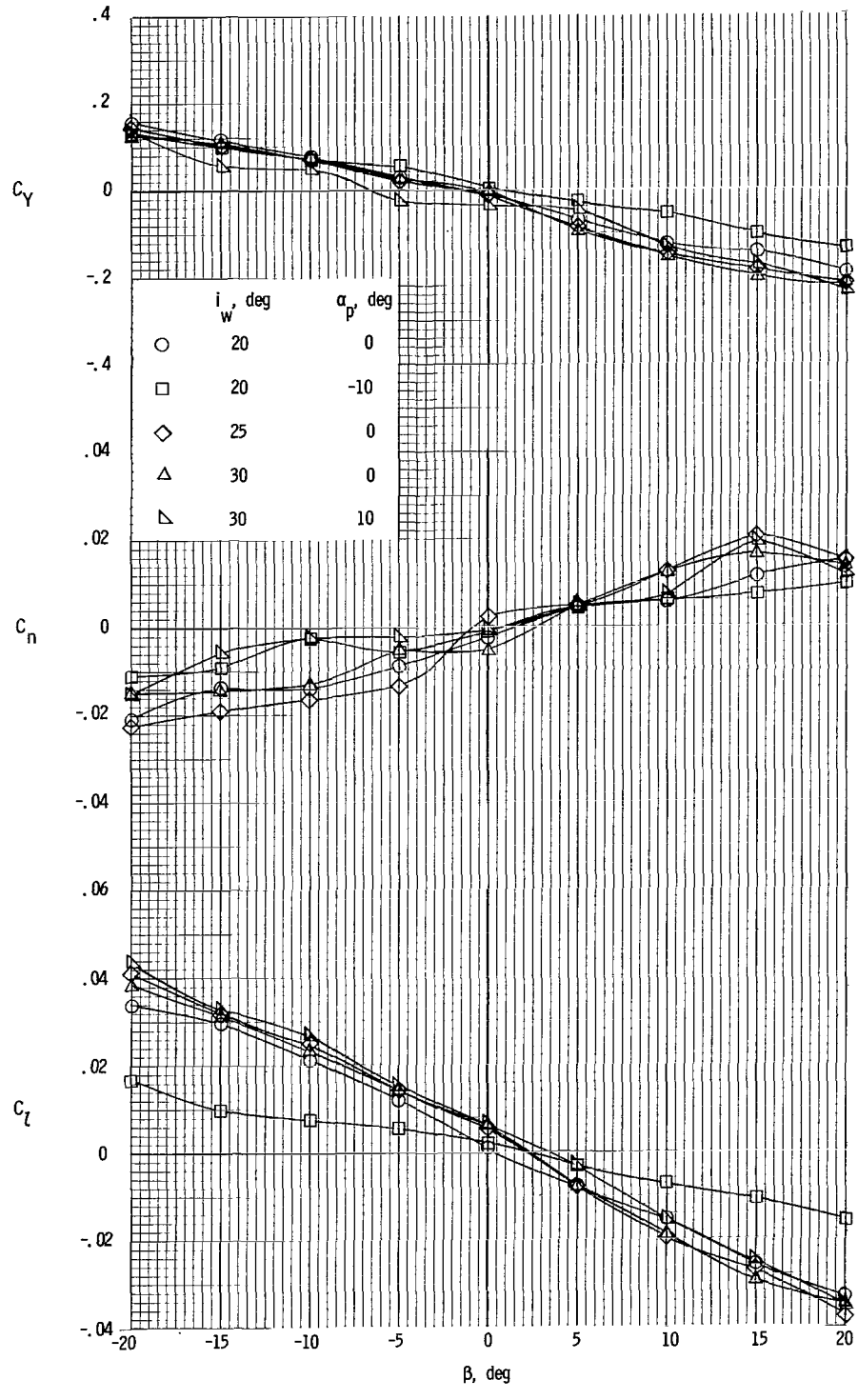

Figure 14.- Static lateral characteristics of model. Design configuration; windmilling propeller; $\delta_e = 0^o$; $\delta_r = 0^o$.

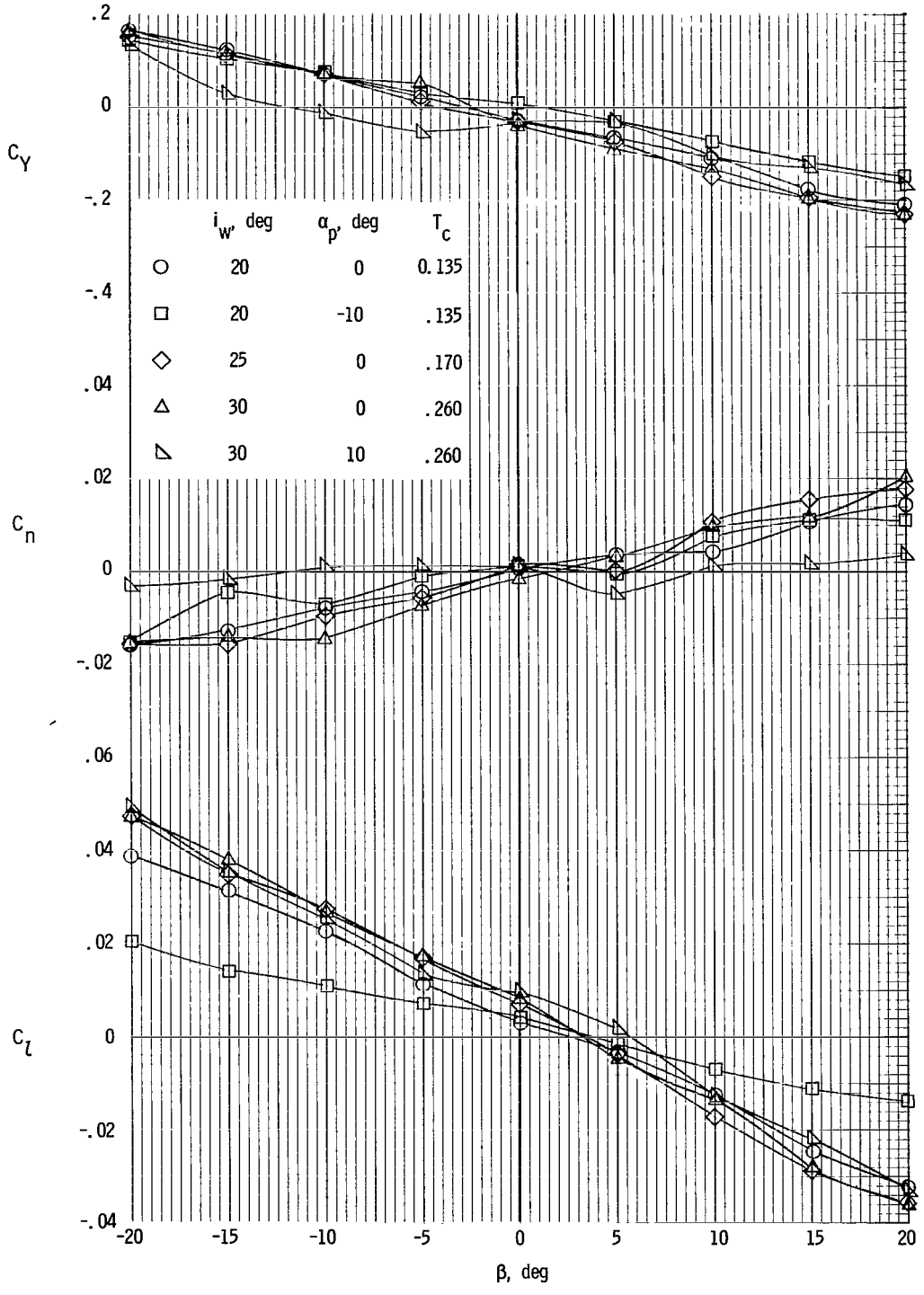

Figure 15.- Static lateral characteristics of model. Design configuration; power on; $\delta_e = 0^o$; $\delta_r = 0^o$.

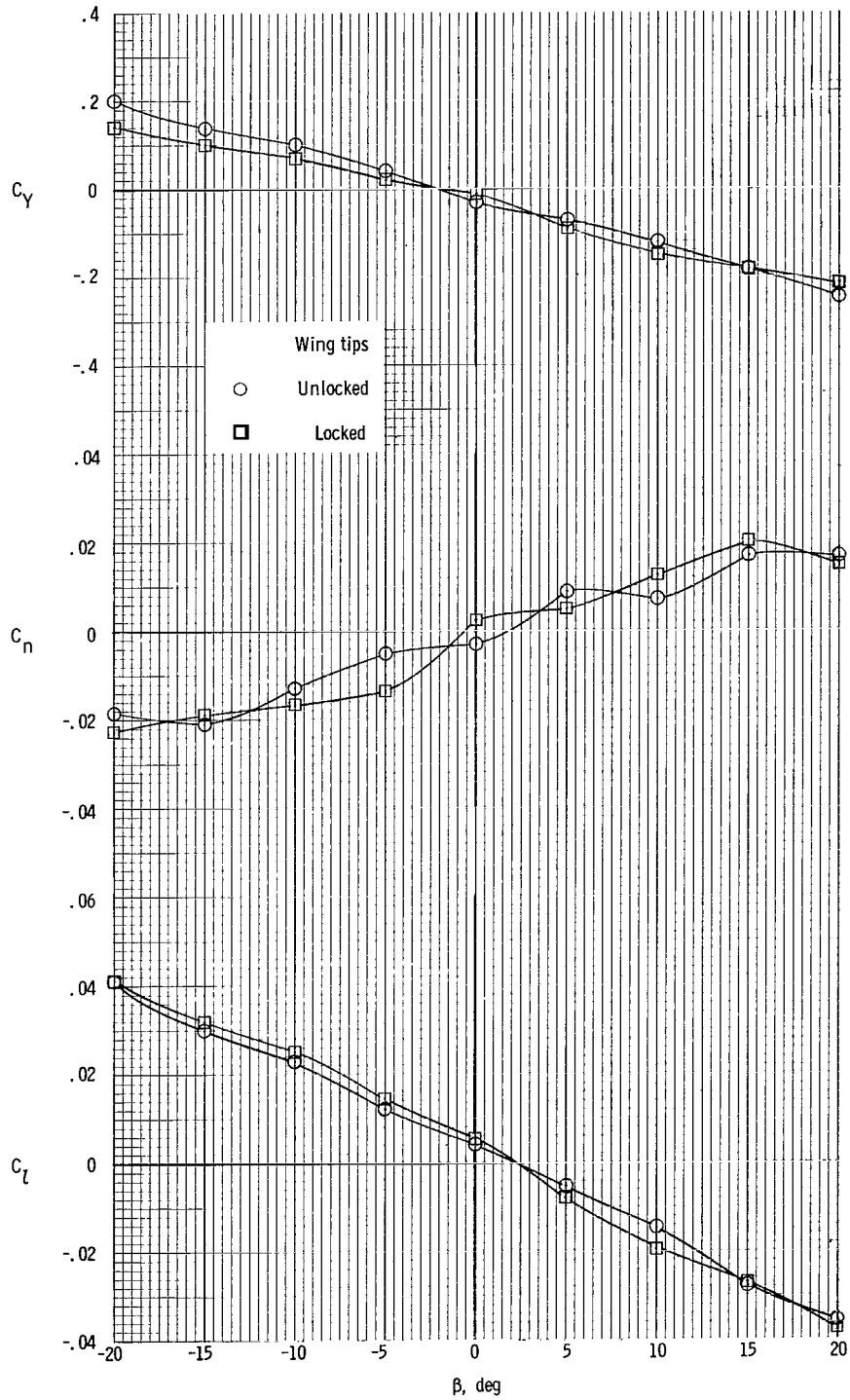

Figure 16.- Comparison of static lateral characteristics of model with wing tips locked and unlocked. Vee-tail on; windmilling propeller; $\delta_e = 0^\circ$; $i_w = 25^\circ$; $\alpha_p = 0^\circ$; $\delta_r = 0^\circ$.

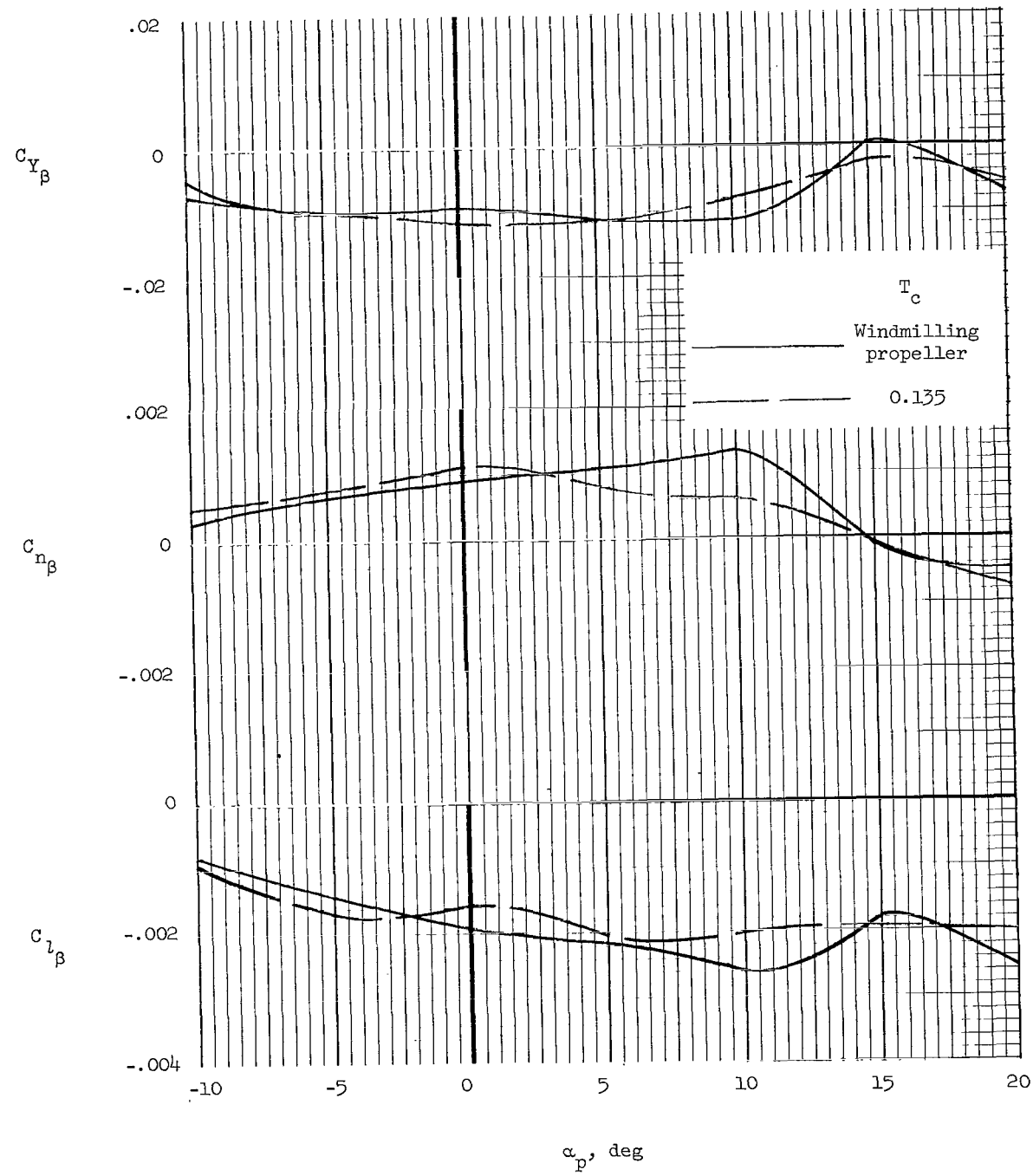

(a) $i_w = 20^\circ$.

Figure 17.- Static lateral stability parameters of model. Design configuration; $\delta_e = 0^\circ$; $\delta_r = 0^\circ$.

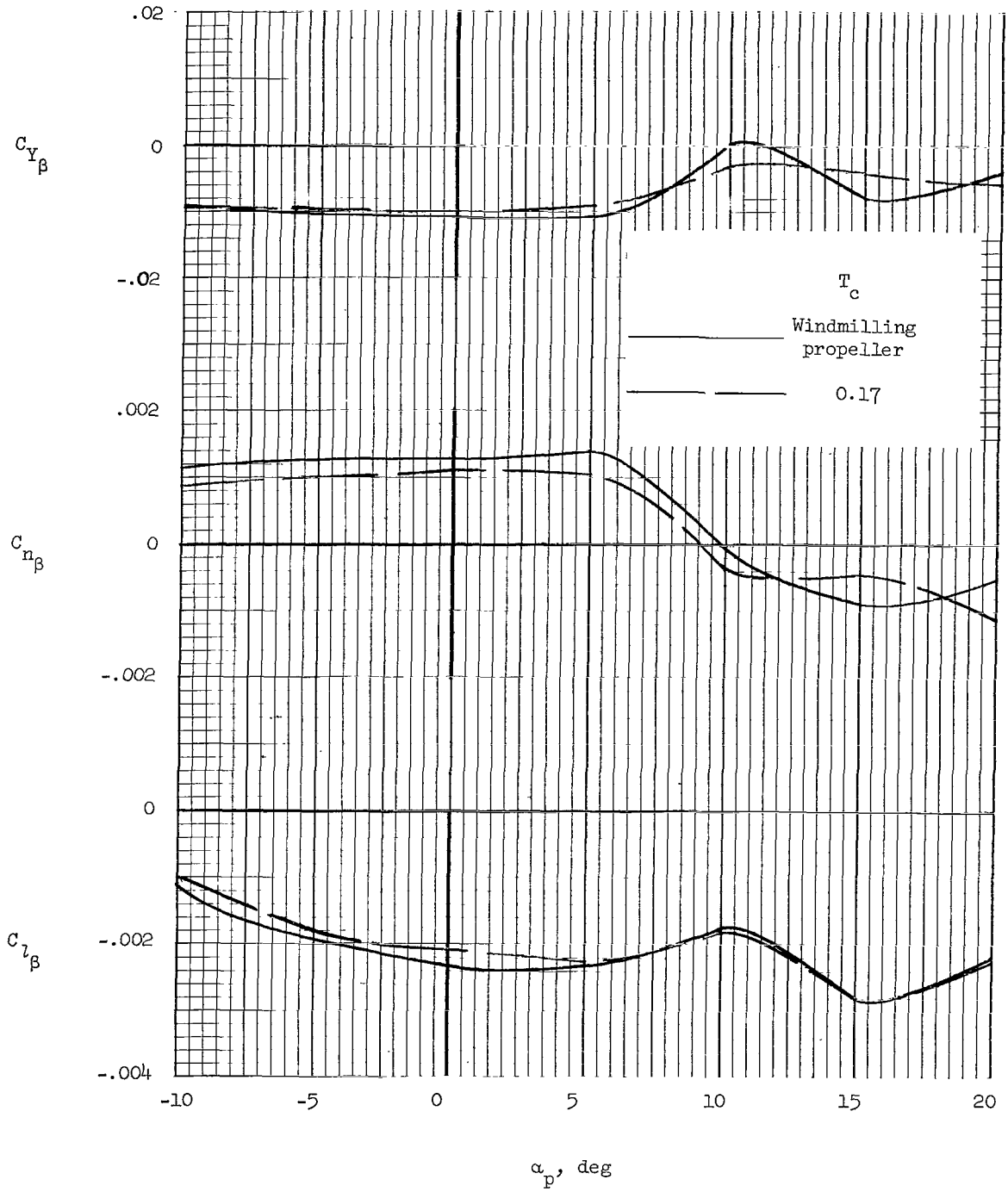

(b) $i_w = 25°$.

Figure 17.- Continued.

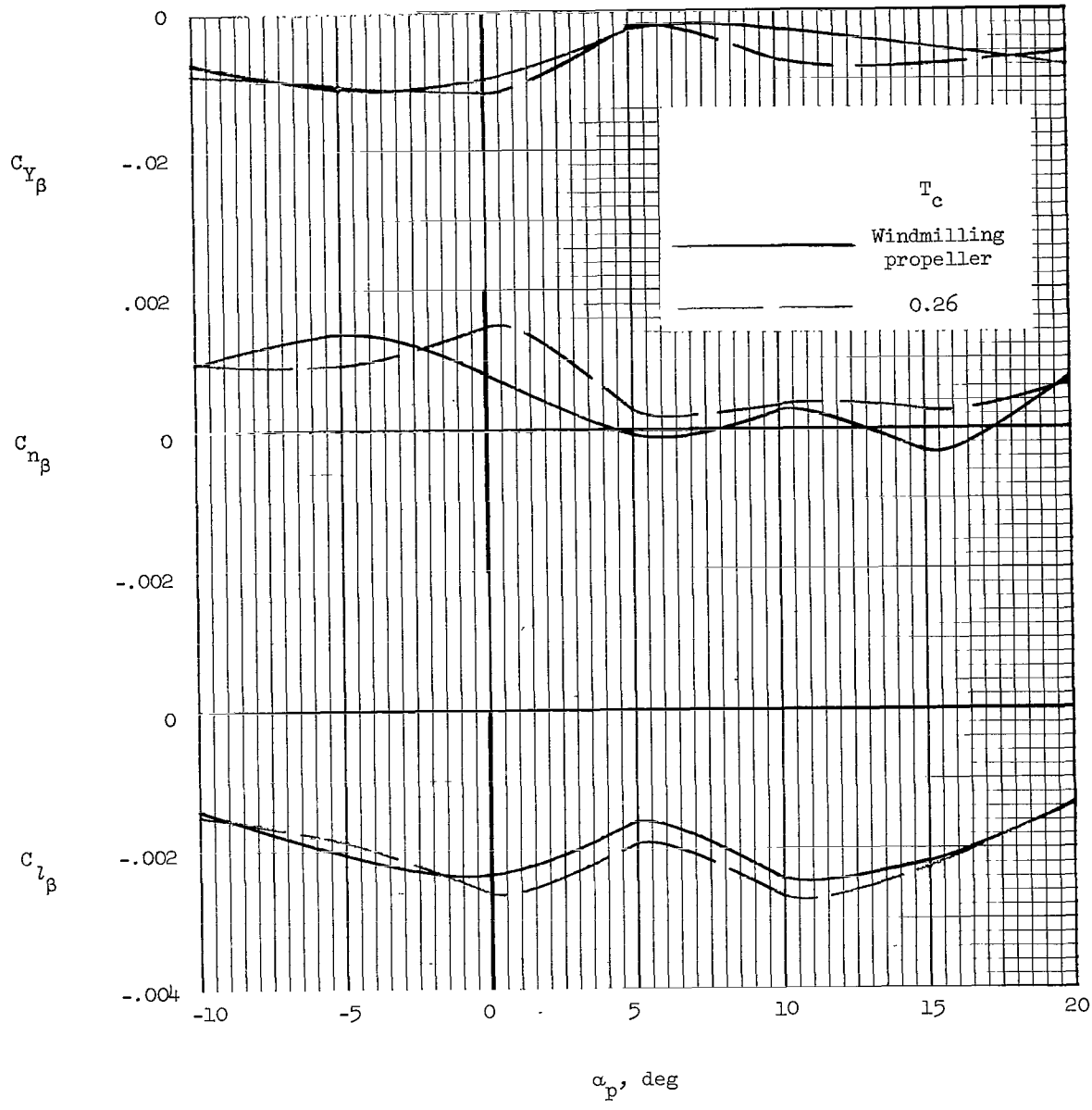

(c) $i_w = 30°$.

Figure 17.- Continued.

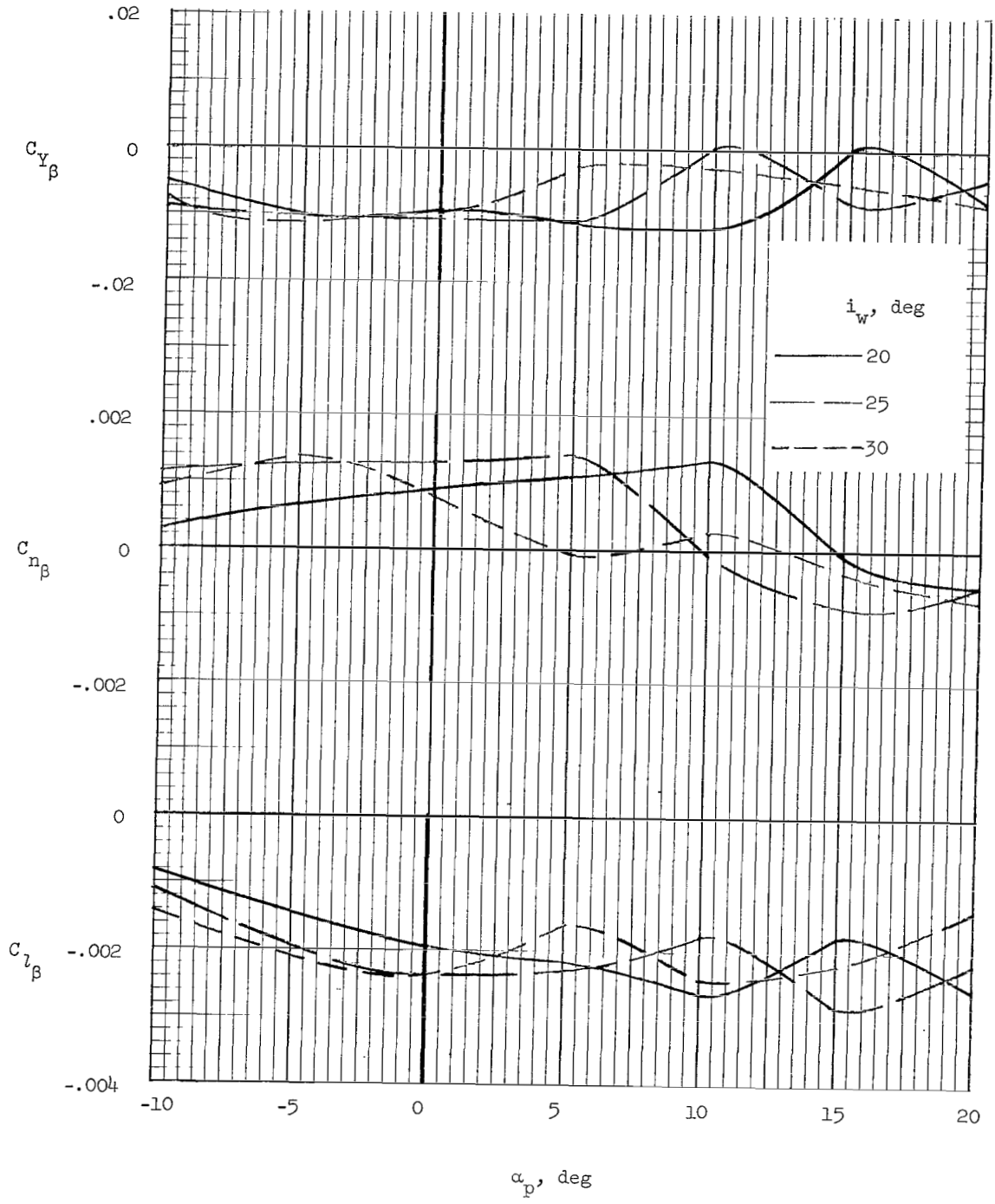

(d) Effect of i_w. Windmilling propeller.

Figure 17.- Concluded.

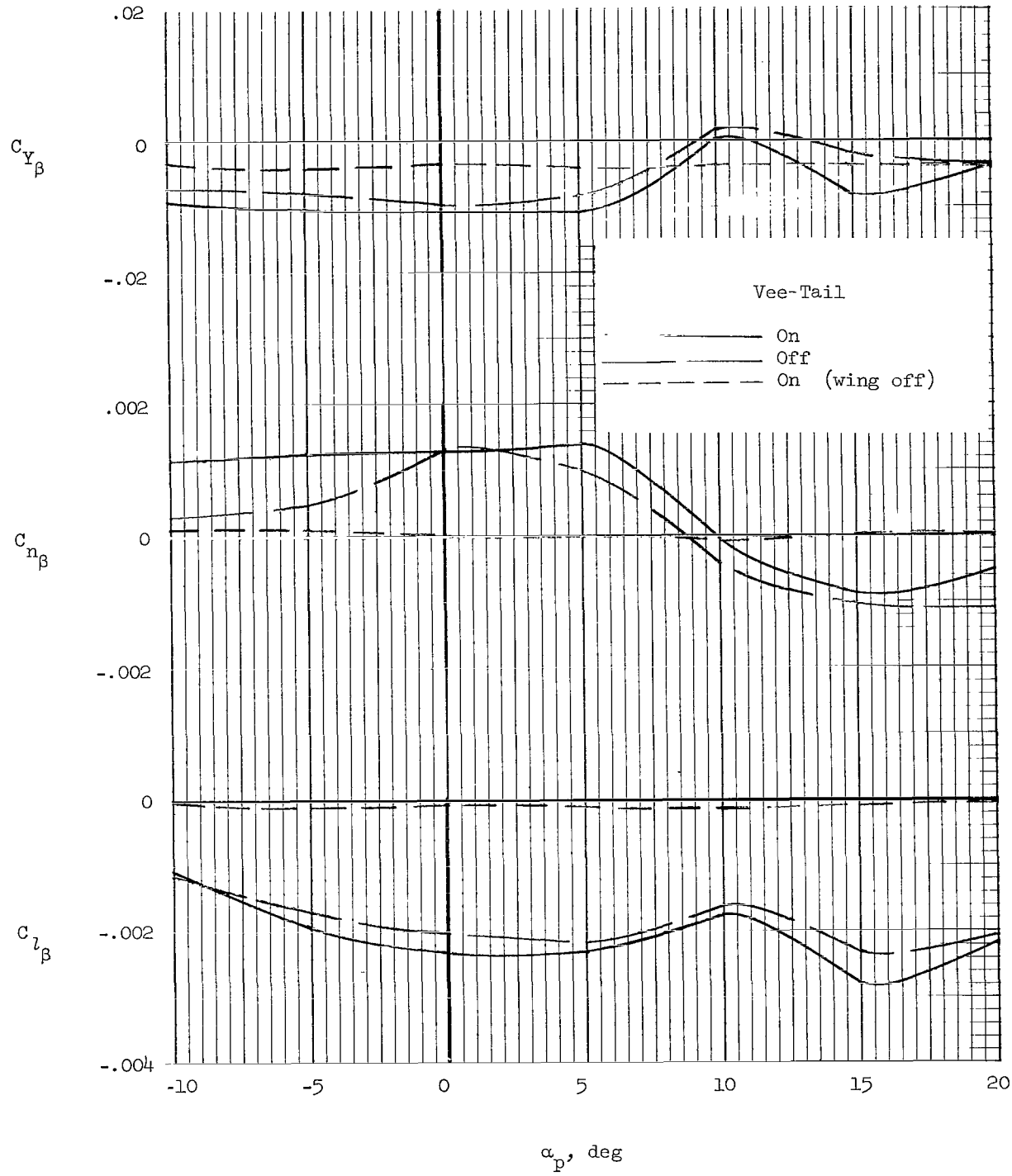

Figure 18.- Effect of vee-tail configuration on static lateral stability characteristics of model. Windmilling propeller; $i_w = 25^\circ$; $\delta_e = 0^\circ$; $\delta_r = 0^\circ$.

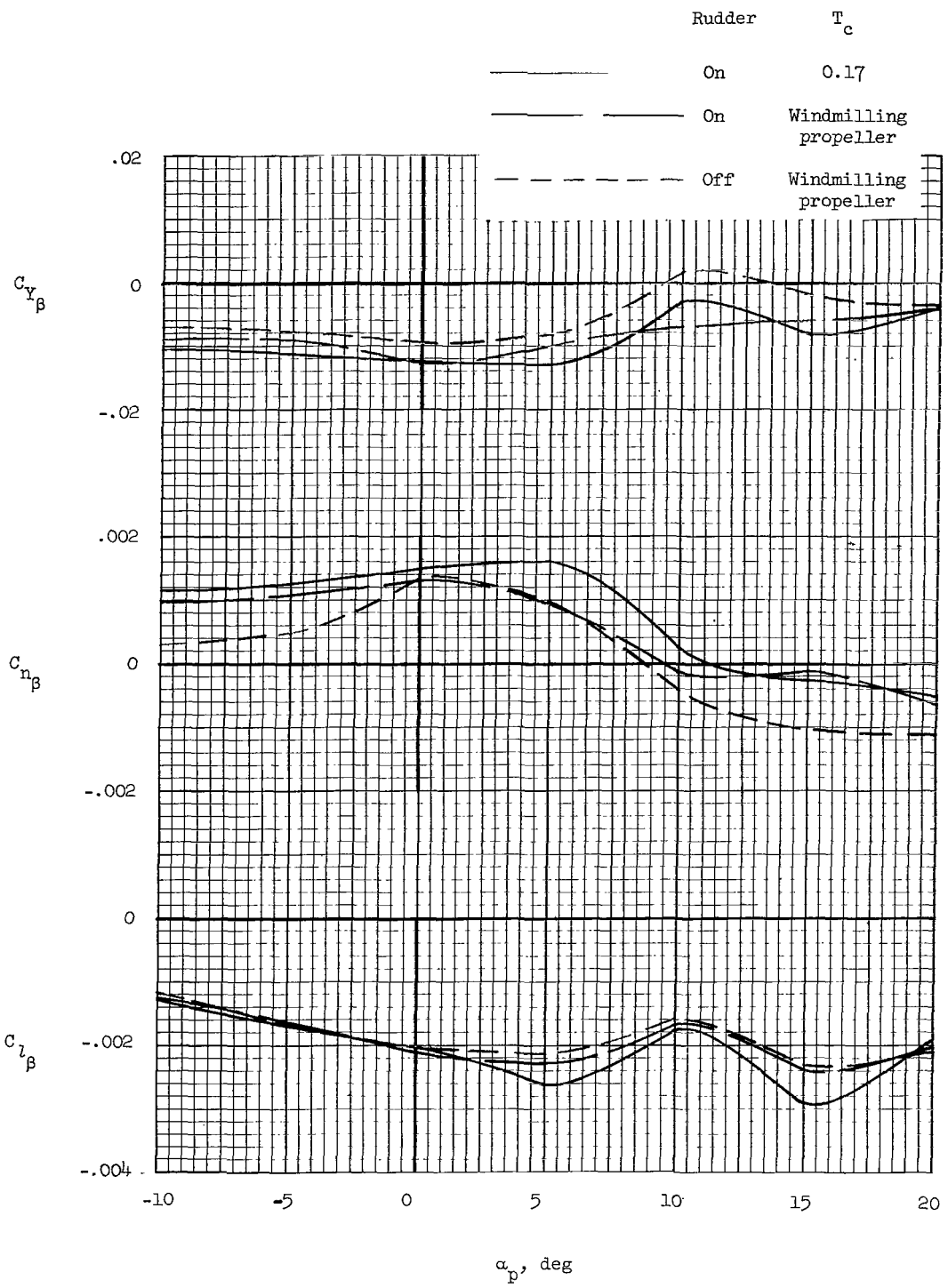

Figure 19.- Effect of vertical rudder surface on static lateral stability characteristics of model. $i_w = 25^\circ$; vee-tail off.

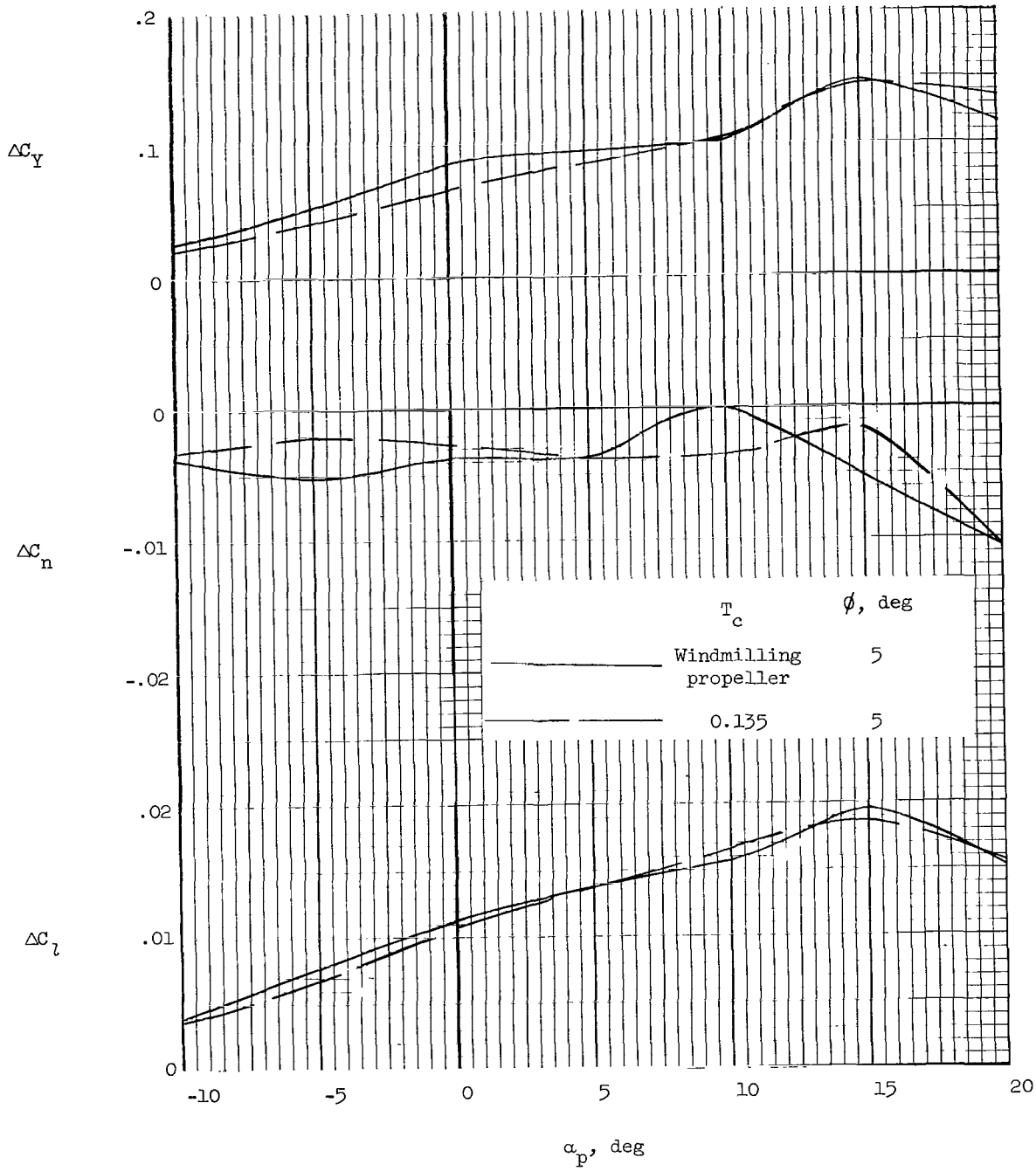

(a) $i_w = 20^o$.

Figure 20.- Incremental lateral forces and moments produced by banking the wing. Design configuration; $\delta_e = 0^o$; $\delta_r = 0^o$.

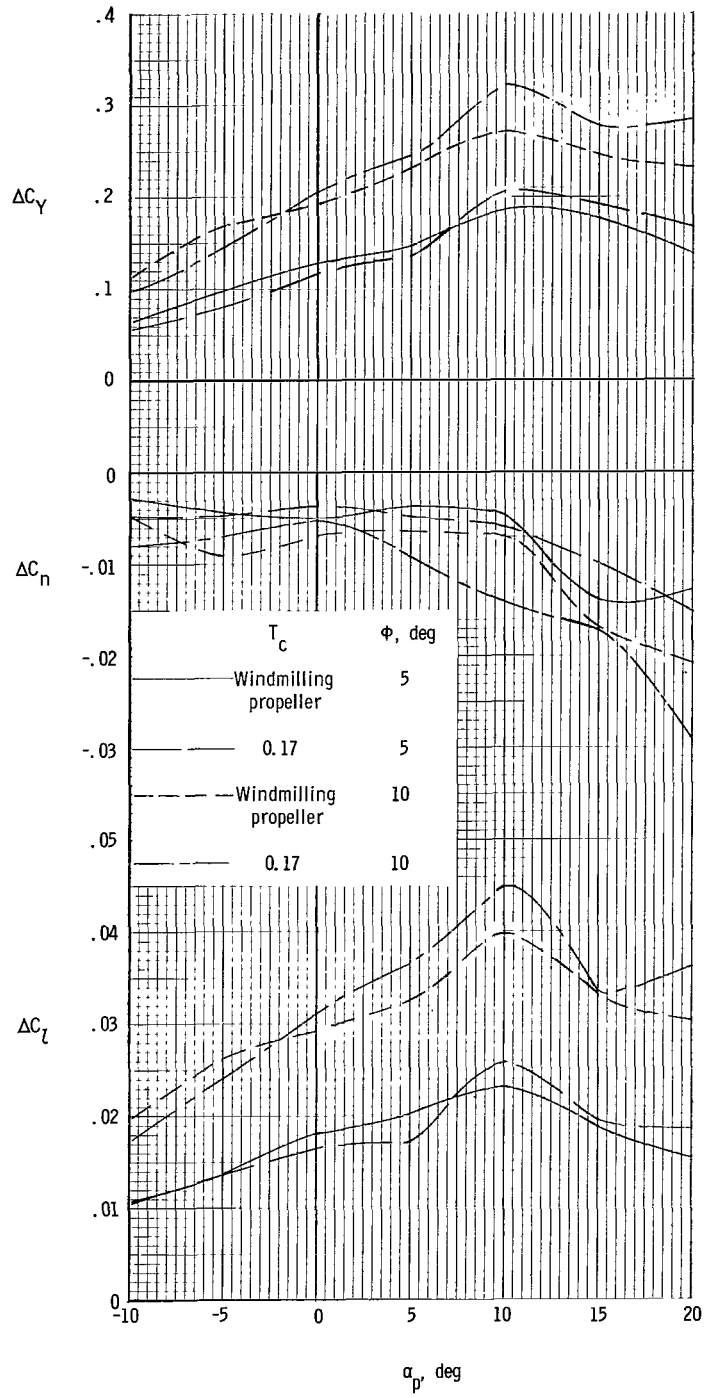

(b) $i_w = 25°$.

Figure 20.- Continued.

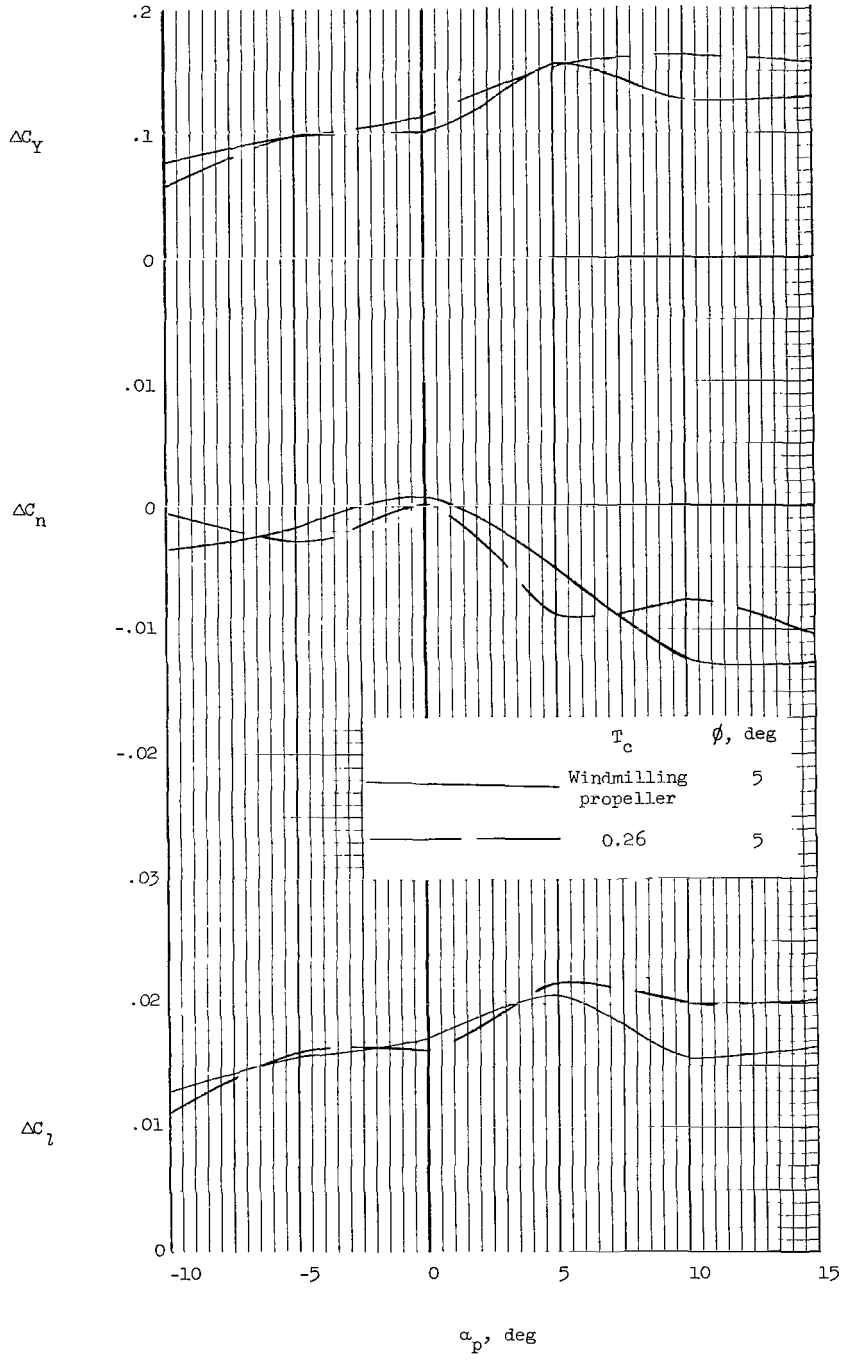

(c) $i_w = 30^o$.

Figure 20.- Concluded.

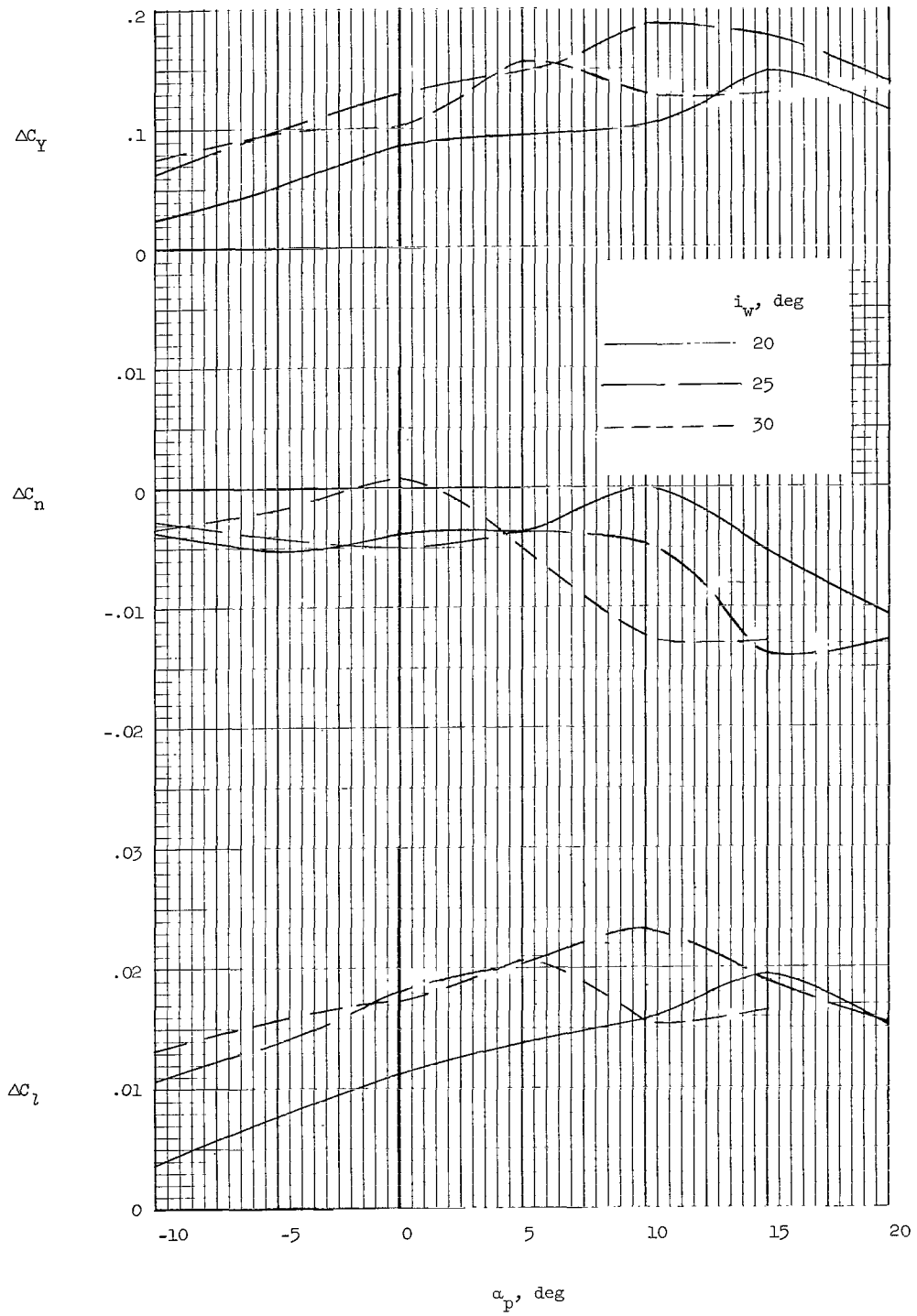

Figure 21.- Comparison of incremental lateral forces and moments produced by banking the wing. Design configuration; windmilling propeller; $\phi = 5^o$; $\delta_e = 0^o$; $\delta_r = 0^o$.

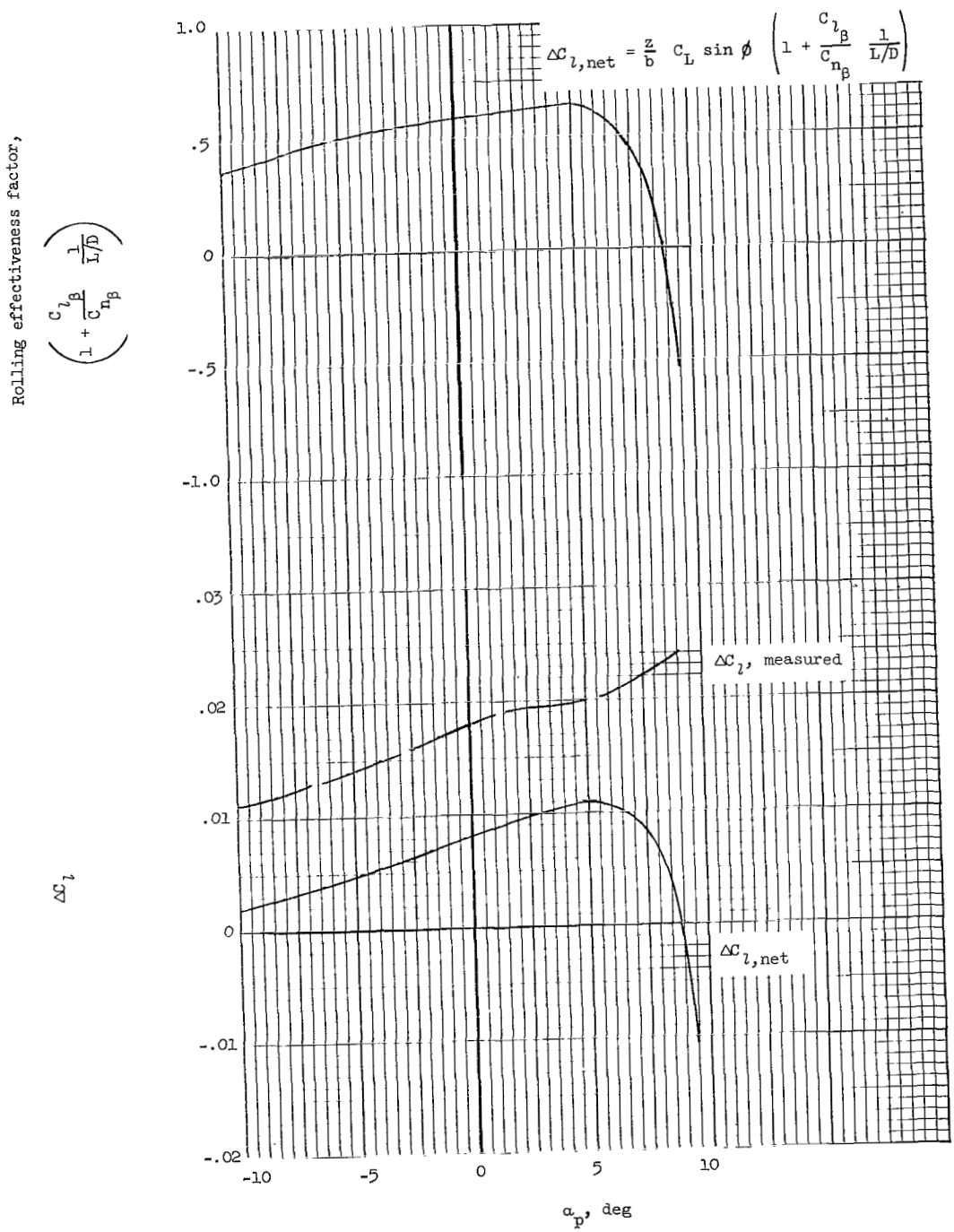

Figure 22.- Comparison of measured rolling moment and calculated net rolling moment produced by banking the wing. (Data referred to stability axis.) Design configuration; windmilling propeller; $i_w = 25^\circ$; $\phi = 5^\circ$; $\delta_e = 0^\circ$; $\delta_r = 0^\circ$.

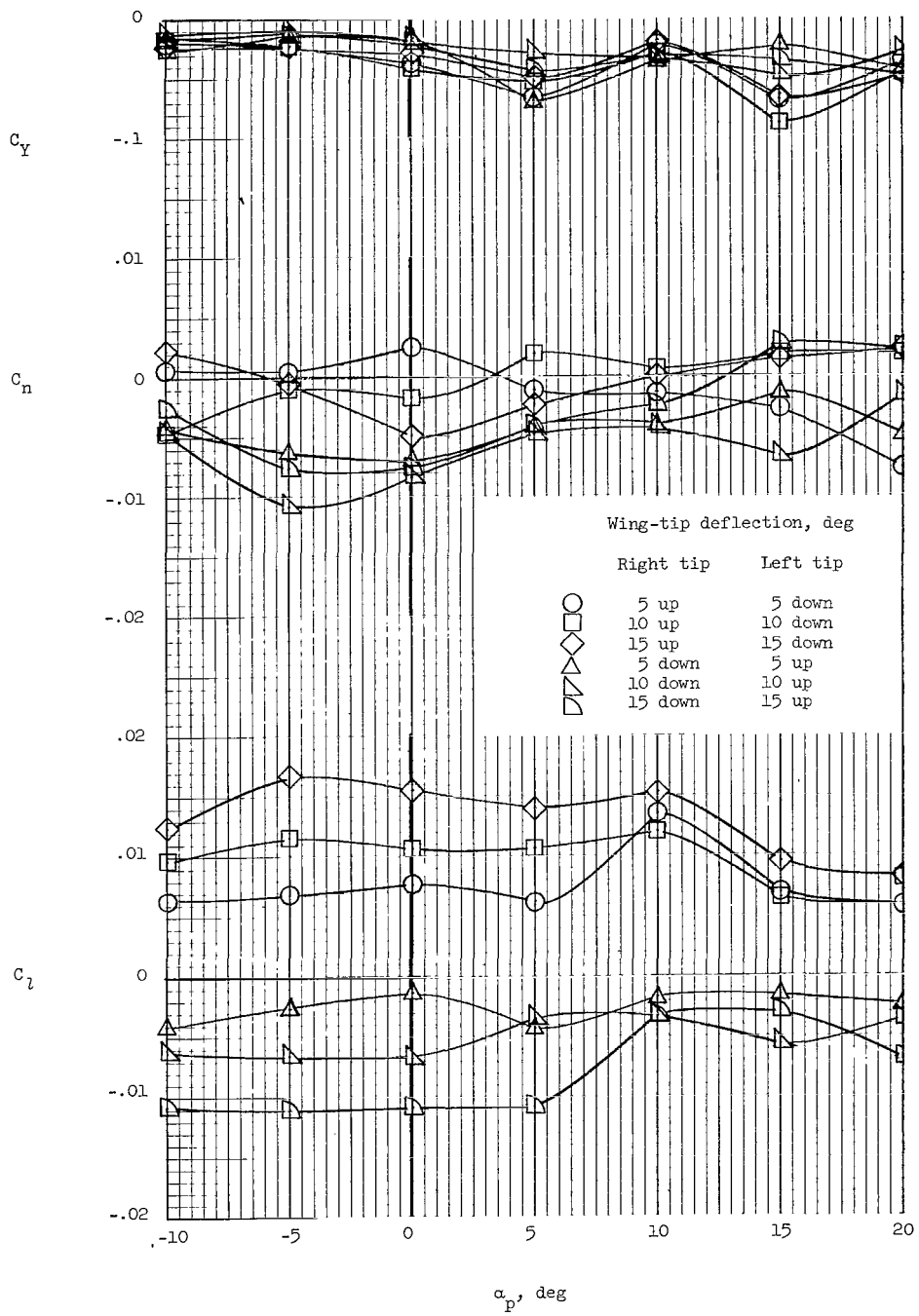

(a) Lateral forces and moments.

Figure 23.- Lateral control characteristics produced by differential deflection of wing tips. Vee-tail on; windmilling propeller; $i_w = 25^\circ$; $\phi = 0^\circ$; $\delta_e = 0^\circ$; $\delta_r = 0^\circ$.

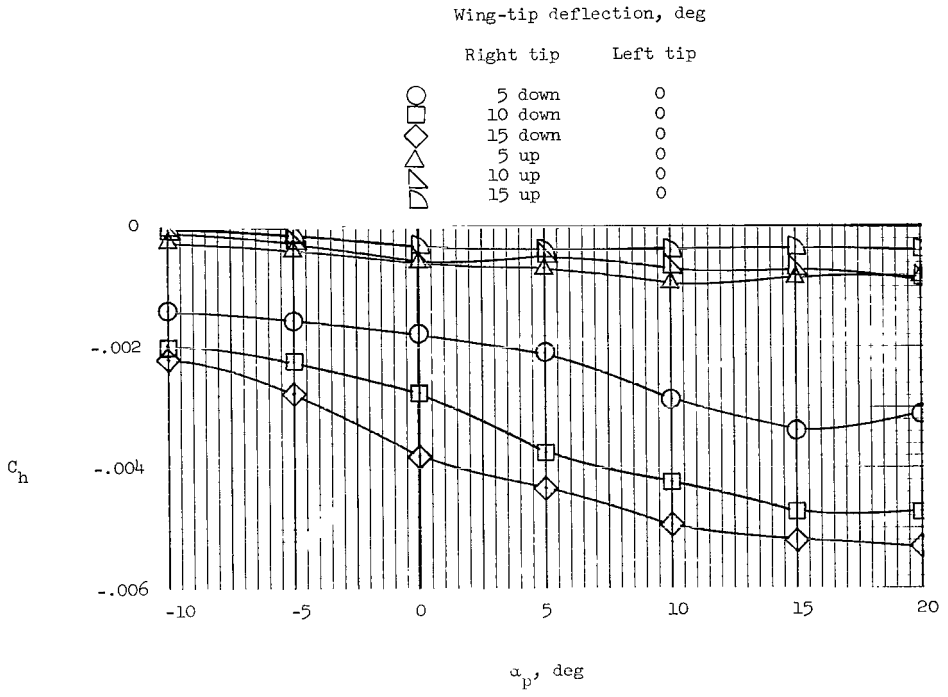

(b) Lateral hinge moments.

Figure 23.- Continued.

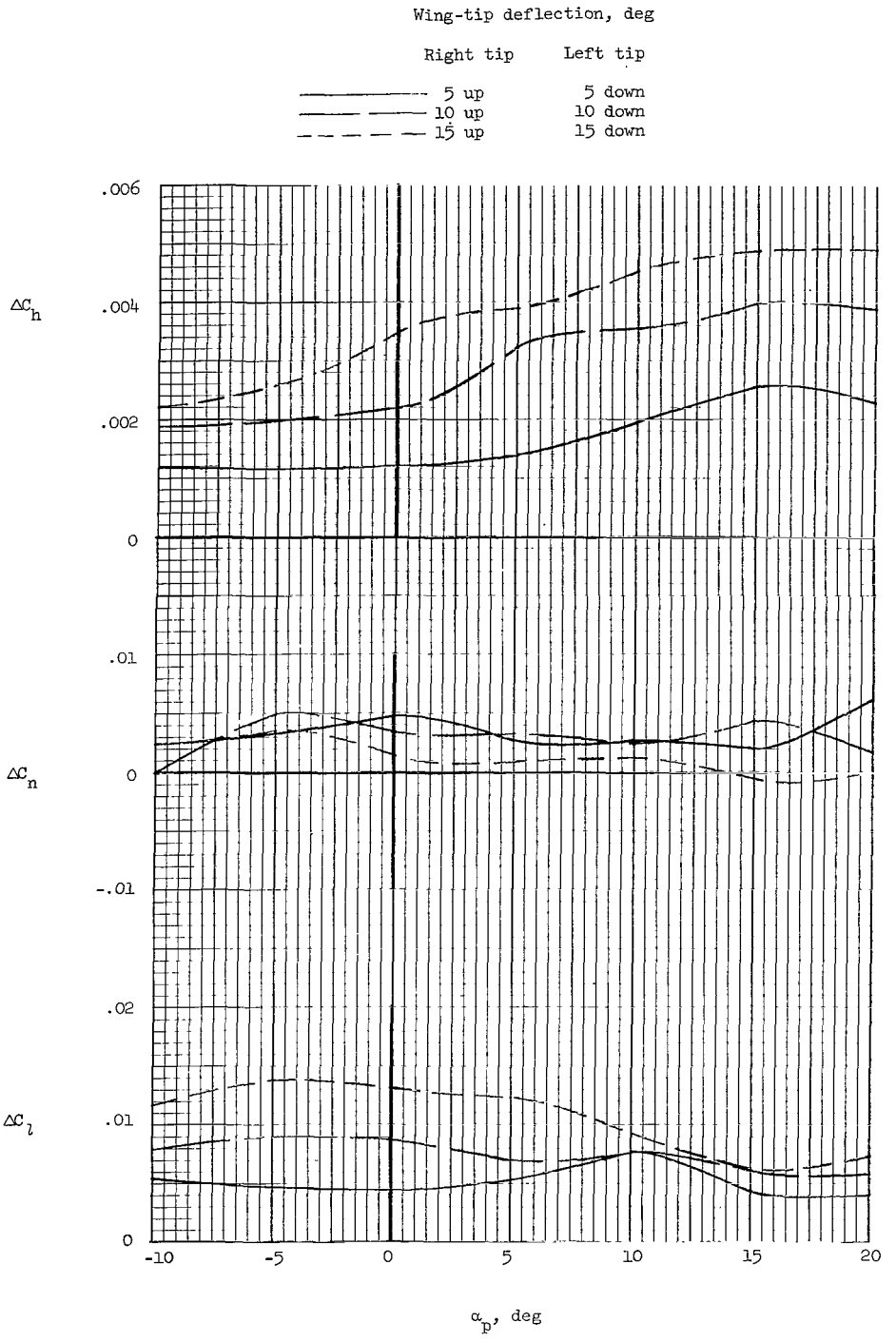

(c) Incremental lateral control characteristics.

Figure 23.- Concluded.

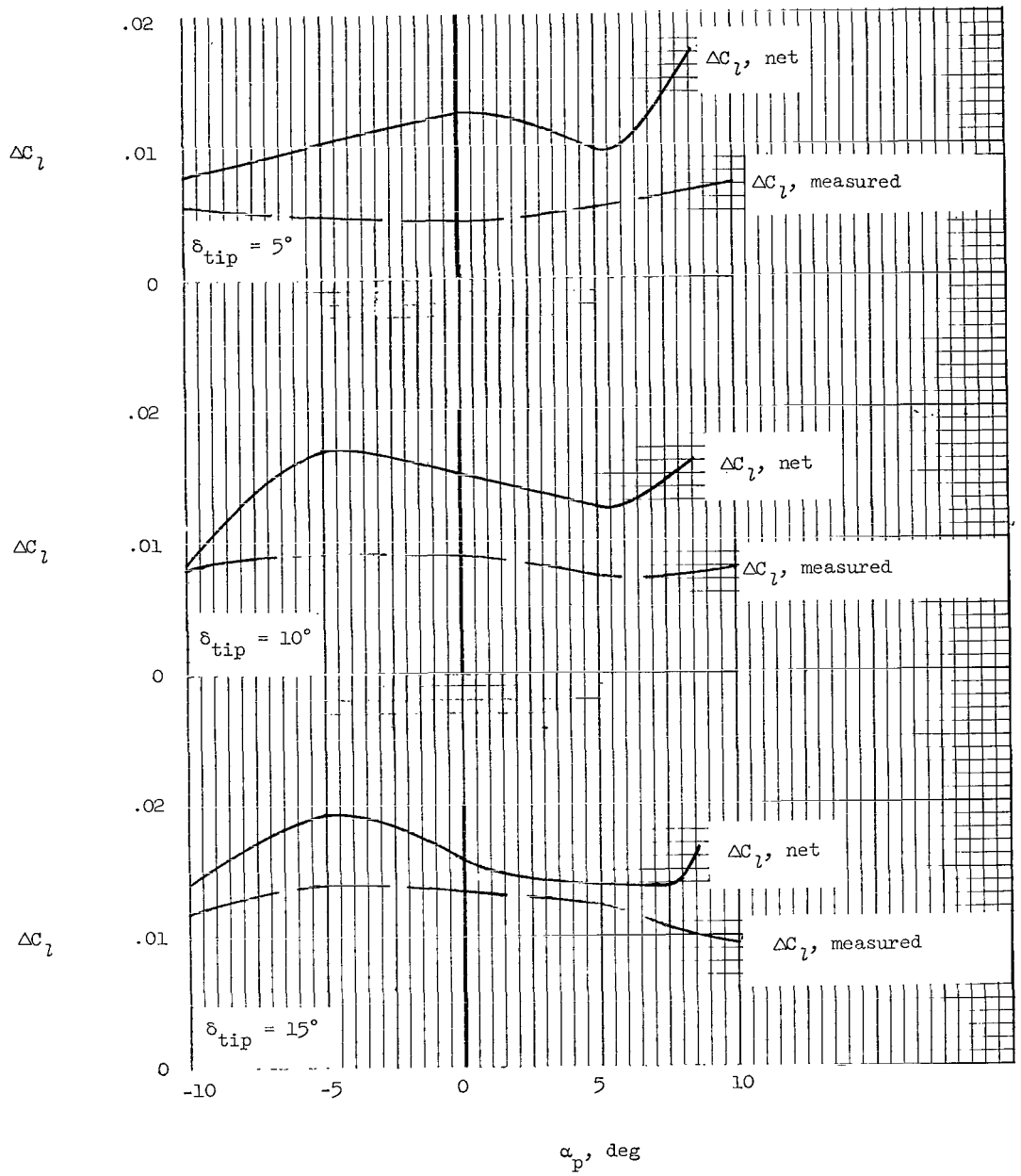

Figure 24.- Comparison of measured rolling moment and calculated net rolling moment produced by wing-tip deflection. Windmilling propeller; $i_w = 25^\circ$; $\phi = 0^\circ$; $\delta_e = 0^\circ$; $\delta_r = 0^\circ$.

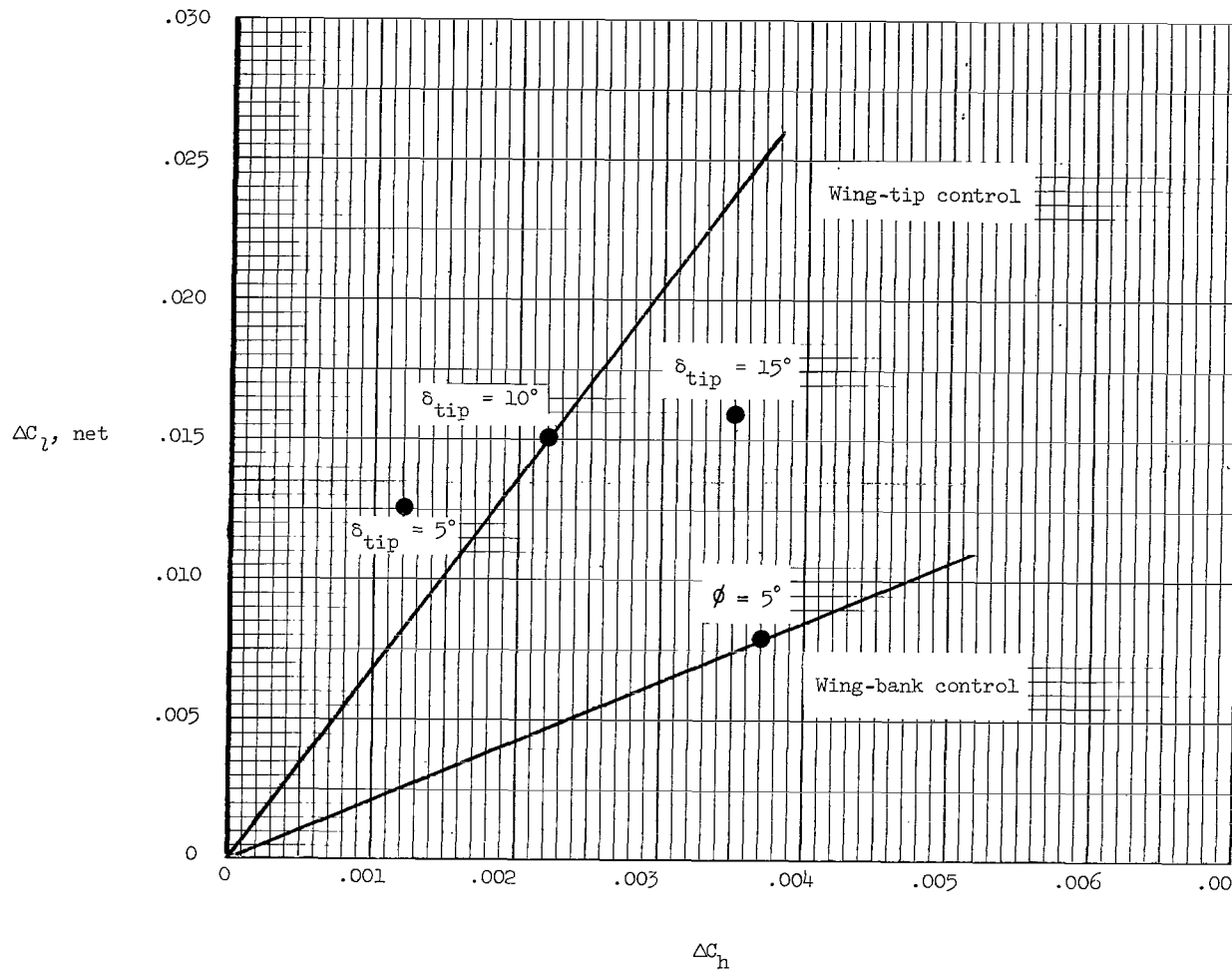

Figure 25.- Comparison of lateral control characteristics of wing-bank control system with those of wing-tip control system. Windmilling propeller; $i_w = 25^\circ$; $\delta_e = 0^\circ$; $\delta_r = 0^\circ$.

δ_r, deg	T_c
-10	Windmilling propeller
-10	0.17
-20	Windmilling propeller
-20	0.17

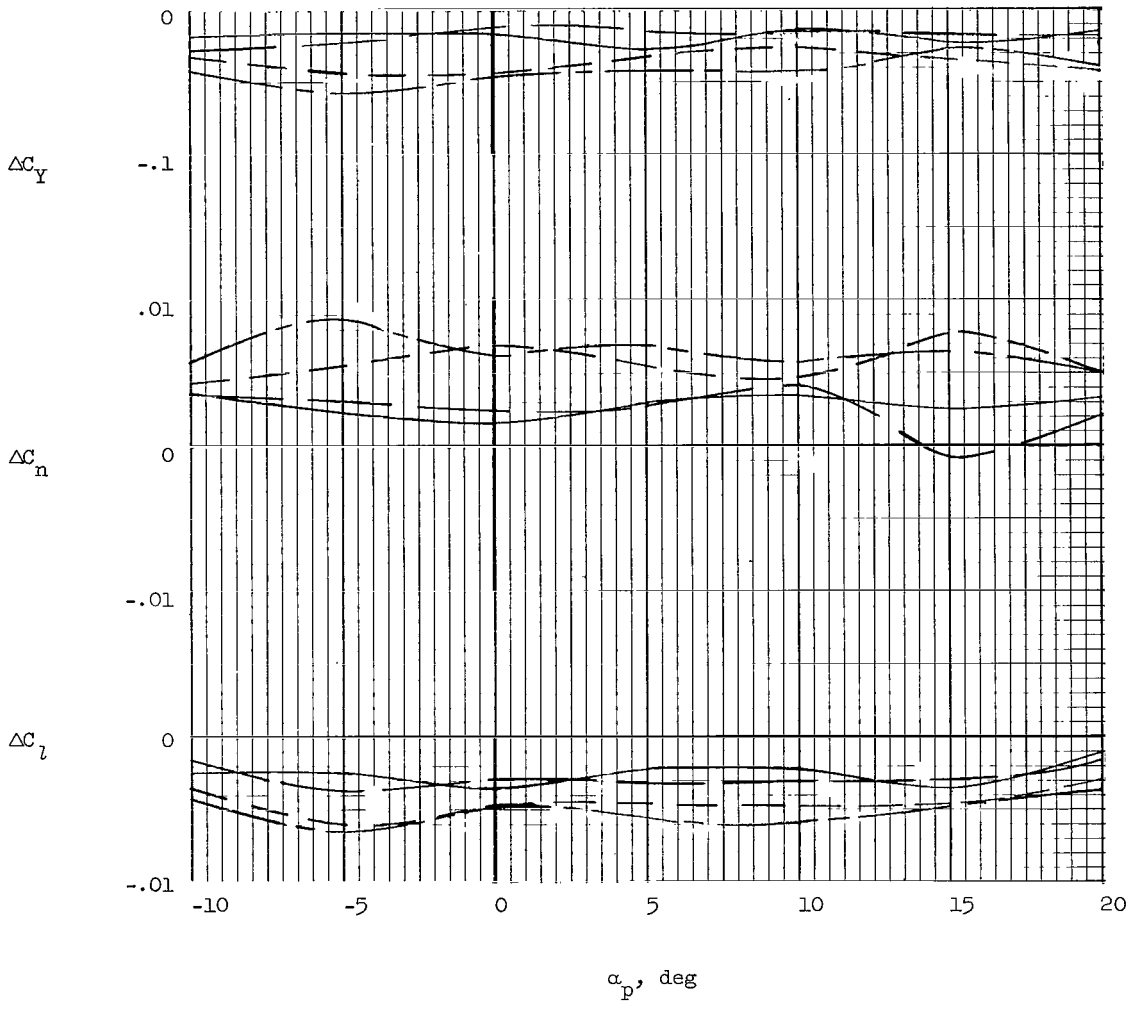

(a) Vee-tail rudders.

Figure 26.- Incremental lateral forces and moments produced by rudder deflection. $i_w = 25^\circ$; $\delta_e = 0^\circ$.

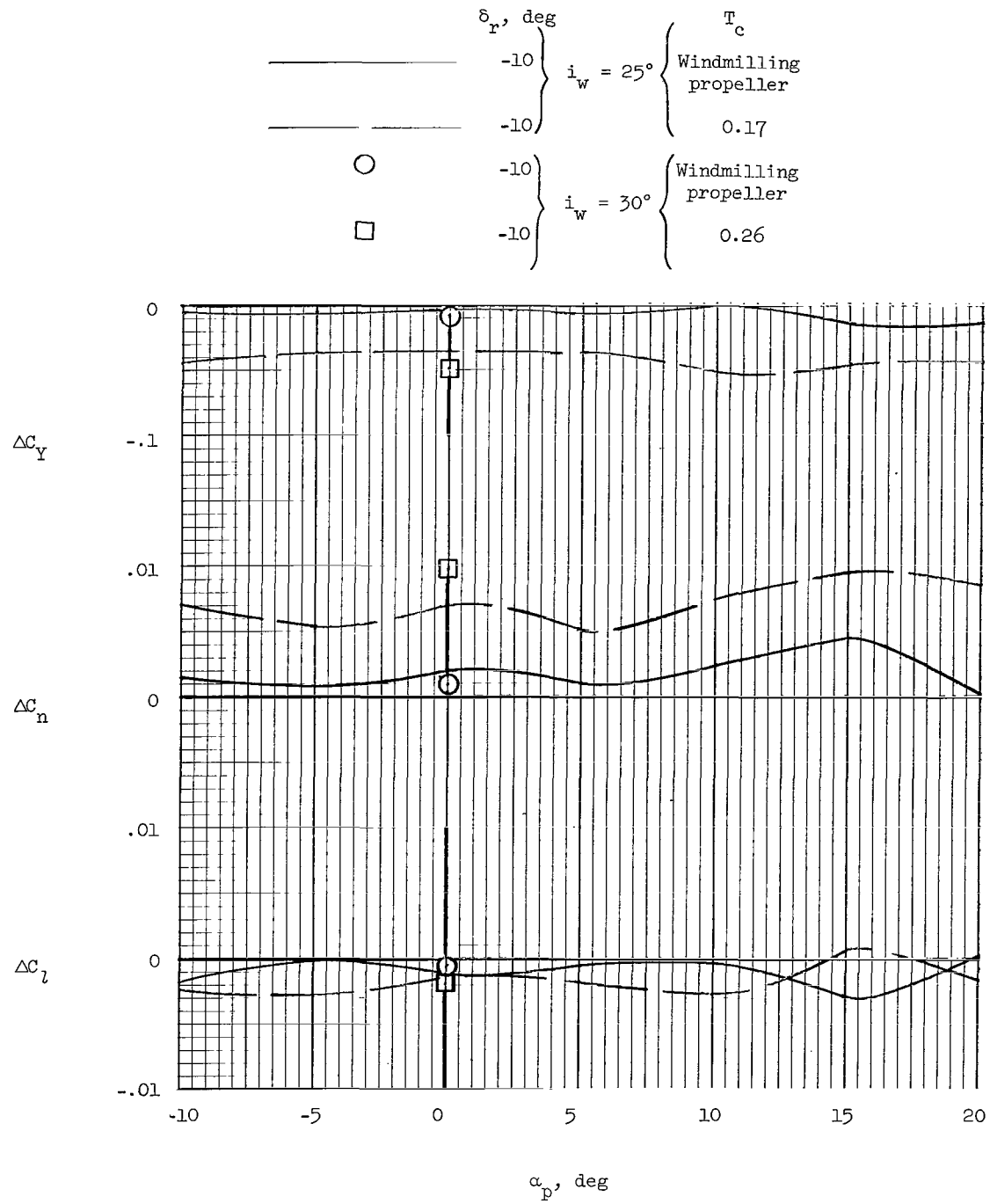

(b) Vertical rudder surface.

Figure 26.- Concluded.

NASA-Langley, 1965 L-4076

A motion-picture film supplement L-836 is available on loan. Requests will be filled in the order received. You will be notified of the approximate date scheduled.

The film (16 mm, 6 min, color, silent) deals with a low-speed wind-tunnel investigation of flight characteristics of a model of a modified parawing utility vehicle. Flight tests were made over an angle-of-attack range of the parawing keel from about 20° to 31°.

Requests for the film should be addressed to:

Chief, Photographic Division
NASA Langley Research Center
Langley Station
Hampton, Va. 23365

C U T

Date _____

Please send, on loan, copy of film supplement L-836 to TN D-2492.

_____
Name of organization

_____
Street number

_____
City and State Zip code

Attention: Mr. _____

Title _____

"The aeronautical and space activities of the United States shall be conducted so as to contribute . . . to the expansion of human knowledge of phenomena in the atmosphere and space. The Administration shall provide for the widest practicable and appropriate dissemination of information concerning its activities and the results thereof."

—NATIONAL AERONAUTICS AND SPACE ACT OF 1958

NASA SCIENTIFIC AND TECHNICAL PUBLICATIONS

TECHNICAL REPORTS: Scientific and technical information considered important, complete, and a lasting contribution to existing knowledge.

TECHNICAL NOTES: Information less broad in scope but nevertheless of importance as a contribution to existing knowledge.

TECHNICAL MEMORANDUMS: Information receiving limited distribution because of preliminary data, security classification, or other reasons.

CONTRACTOR REPORTS: Technical information generated in connection with a NASA contract or grant and released under NASA auspices.

TECHNICAL TRANSLATIONS: Information published in a foreign language considered to merit NASA distribution in English.

TECHNICAL REPRINTS: Information derived from NASA activities and initially published in the form of journal articles.

SPECIAL PUBLICATIONS: Information derived from or of value to NASA activities but not necessarily reporting the results of individual NASA-programmed scientific efforts. Publications include conference proceedings, monographs, data compilations, handbooks, sourcebooks, and special bibliographies.

Details on the availability of these publications may be obtained from:

SCIENTIFIC AND TECHNICAL INFORMATION DIVISION

NATIONAL AERONAUTICS AND SPACE ADMINISTRATION

Washington, D.C. 20546